**Quaternary Science Reviews**
August 2021, Volume 265 Pages 107050 (14p.)
https://doi.org/10.1016/j.quascirev.2021.107050
https://archimer.ifremer.fr/doc/00704/81644/



# Orbital forcing in southern Africa: Towards a conceptual model for predicting deep time environmental change from an incomplete proxy record

Chase Brian M. [1, 2, *]

[1] Institut des Sciences de L'Evolution-Montpellier (ISEM), University of Montpellier, Centre National de La Recherche Scientifique (CNRS), EPHE, IRD, Montpellier, France
[2] Department of Environmental and Geographical Science, University of Cape Town, South Lane, Upper Campus, 7701 Rondebosch, South Africa

* Corresponding author : Brian M. Chase, email address : brian.chase@umontpellier.fr

**Abstract :**

Southern Africa hosts regions of exceptional biodiversity and is rich with evidence for the presence and activities of early humans. However, few records exist of the concurrent changes in climate that may have shaped the region's ecological evolution and the development and dispersal of our ancestors. This lack of evidence limits our ability to draw meaningful inferences between important changes in the global and regional climate systems and their potential influence in shaping the region's natural and cultural history. This paper synthesises the data currently available to define a general empirically-based conceptual model of the spatio-temporal dynamics of climate change as they relate to changes in the earth's orbital configurations. The goal is to identify mechanistic links between orbital forcing, which can be calculated continuously over the past several million years, and environmental responses to related changes in the major atmospheric and oceanic circulation systems influencing southern Africa. Once identified, these relationships can be used to infer the most likely trends and patterns of climate variability for periods and regions for which proxy evidence is not available.

Findings indicate that coherent patterns of change can be observed at wavelengths associated with ~400-kyr and ~100-kyr cycles of orbital eccentricity. In southeastern Africa, the ~2400-kyr grand cycle in eccentricity may have had an influence long-term patterns of aridification and humidification, and the stronger ~400-kyr eccentricity cycle has a significant influence across inter-tropical Africa, through changes in hydroclimate and monsoon circulation. The attribution of the ~100-kyr cycle to specific orbital controls depends on location, as it can be determined by eccentricity-modulated direct insolation forcing or through the combined orbital parameters and earth system responses that drive the evolution of Pleistocene glacial-interglacial cycles.

Following the onset of the mid-Pleistocene transition (c. 1250–700 ka), the increasing development of substantial polar ice sheets influence the nature of high-latitude drivers in southern Africa. In southwestern Africa, records indicate an evolution in climate and circulation systems strongly correlated with the global benthic δ18O record, suggesting a particular sensitivity to high latitude forcing. The close correlation between ~100-kyr eccentricity and glacial-interglacial cycles makes it difficult to determine whether high- or low-latitude drivers dominate in southeastern Africa, but the spatio-temporal patterning of environmental variability in many records are generally considered to indicate a degree of high-latitude influence. Records from southeastern and southernmost Africa also indicate that the influence of low latitude forcing, expressed through the local precessional cycle, is – at least over the last glacial-interglacial cycles - dependent on eccentricity. Periods of reduced eccentricity, particularly during periods of extensive high-latitude ice sheet development, result in diminished influence in direct forcing and an increase in the expression of high latitude forcing, and an increasingly positive correlation between the northern and southern tropics at these wavelengths. In general, the records available allow for a simple conceptual model of the relationship between orbital parameters and regional climates to be defined, with the strongest relationships existing at longer timescales, such as the ~400-kyr eccentricity cycle. At finer spatio-temporal timescales, the data indicate degrees of complexity that are not readily predicted, but the expansion of the regional dataset will continue to allow for refinements to the conceptual model described.

**Highlights**

► Review of influence of orbital forcing on southern African palaeo-records. ► Wavelet and semblance analysis used to explore nature of orbital influence. ► Orbital eccentricity has significant influence across inter-tropical Africa. ► Increased ice volume alters climate change dynamics associated with orbital forcing. ► Orbital parameters may be used to infer past conditions when direct evidence is not available.

**Keywords** : Orbital forcing, Milankovitch, Southern Africa, Palaeoclimate, Quaternary, Pliocene

# Introduction

Knowledge of past environmental change in southern Africa is fundamentally limited by a lack of evidence. This is largely due to southern Africa's arid to semi-arid environment, which hinders the development of permanent lakes south of ~15°S. Without such perennial, protected sediment traps, terrestrial records are rare. Where records have been recovered, they are often discontinuous and poorly dated (see Chase and Meadows, 2007). Only three terrestrial records from the region, from Lake Malawi (Johnson et al., 2016), Tswaing Crater (Partridge et al., 1997) and Pinnacle Point (Braun et al., 2019) encompass more than the last glacial-interglacial cycle (125 kyr). Broader inferences relating to the influence of orbital forcing on regional climates may thus only be drawn from 1) proxy data recovered from marine records, which may preserve longer sedimentary sequences of both marine and terrestrial origin, and 2) by extrapolation of relationships observed between these data and terrestrial records from more recent portions of the geological record. Further complicating this research is the recognition that prevailing conceptual models for regional climate change only have limited predictive capabilities, and that significant variability is the result of more complex processes (e.g. Chase et al., 2017), resulting in substantially greater spatio-temporal heterogeneity in signals of environmental change (Chase et al., in press; Chase et al., 2019a; Chase and Quick, 2018; Chevalier and Chase, 2015).

This paper reviews: 1) the general framework of the southern African climate systems that are considered to have driven the major trends in environmental variability during the late Quaternary, and 2) how mechanisms both external (i.e. orbital parameters) and internal (e.g. continental ice sheets, $CO_2$) to the earth system may influence these systems. The goal is to provide a general model for the use of orbital parameters to infer past climate conditions and trends for periods from which proxy data is not available.

## Southern African climate systems

Southern Africa (considered to be 0°-35°S for the purpose of this paper) experiences much greater climatic diversity than its Northern Hemisphere counterpart (Peel et al., 2007). This is due to a series of factors related to the continent's morphology and latitudinal position. While northern Africa is, with the addition of the Arabian Peninsula, nearly 8,000 km across from east to west, southern Africa is just over 3,000 km across. This relatively small area limits the development of high pressure over the continent and enables the effective incursion of moist air from the adjacent tropical Indian and Atlantic oceans. In the east, the warmth of the Agulhas Current fosters increased evaporation and the transport of moisture into the interior (Crétat et al., 2012; Rouault et al., 2002; Tyson and Preston-Whyte, 2000). In the west, tropical moisture advection from the Atlantic Ocean is generally limited to regions north of ~15°S (Crétat et al., 2019; Rouault et al., 2003). Further south, the cold Benguela Current flows equatorward along the South African and Namibian coasts, limiting evaporation and supressing convection (Nicholson and Entekhabi, 1987; Tyson, 1986). As a result, a marked east-west rainfall gradient exists across the subcontinent at these latitudes, and the dominant moisture-bearing systems are northerly flow over Angola and easterly flow from the Indian Ocean. Southern African climates are also strongly influenced by extra-tropical systems. Poleward of the subcontinent, the southern westerlies dominate mid-latitude atmospheric circulation. Perturbations in the westerlies create fronts that produce the majority of rainfall received by the southwestern Cape (Reason et al., 2002). The influences of these various systems have strong seasonal biases, with the tropical systems being most vigorous in the warm summer months, and the extra-tropical frontal systems being most prevalent during the winter, when the Antarctic anticyclone expands and the zone of frontal activity is displaced equatorward (Figure 1).

The diversity and distribution of atmospheric and oceanic circulation systems influencing southern Africa has led to regional distinctions based on the seasonal distribution of rainfall, with most of the subcontinent comprising the summer rainfall zone (SRZ), and the extreme southwestern margin being referred to as the winter rainfall zone (WRZ) (Figure 1). Between the SRZ and the WRZ is a transitional zone, which is influenced by both tropical and temperate systems. This has been referred to variously as the year-round rainfall zone (YRZ), all-year rainfall zone or aseasonal rainfall zone (ARZ). The criteria by which these regions have been defined varies, but a commonly employed method is the percentage of mean annual rainfall during the winter (>66% = WRZ, <33% = SRZ, 33%-66%=YRZ/ARZ; sensu Chase and Meadows, 2007)(Figure 1). Climates in each of these broad regions are highly variable, ranging significantly in terms of the amount of mean annual precipitation received, but the purpose of their definition is to delimit the spatial influence of southern Africa's dominant moisture-bearing systems and thereby develop mechanistic models for their past variability.

## Orbital mechanisms driving long-term climate variability in southern Africa

At their broadest scale, Quaternary climate dynamics are understood to be paced by changes in the Earth's orbital parameters (Berger et al., 1984; Chappell, 1973; Hays et al., 1976; Imbrie, 1982; Imbrie et al., 1984; Milankovitch, 1930). These changes include the shape of the Earth's orbit (eccentricity), the degree of Earth's axial tilt (obliquity) and the direction of the axis at a defined point of Earth's motion around the sun (precession). Each of these parameters varies at quasi-regular cycles: eccentricity expressing ~400,000-year and ~100,000-year cycles, obliquity expressing a ~41,000-year cycle, and precession expressing a ~23,000-year cycle. Respectively, these variables influence the amount of solar insolation the Earth receives, the intensity of the seasons, and the season in which the Earth is closest to the sun and receiving the most insolation. While it is generally accepted that these orbital changes have paced the timing and amplitude of the glacial and interglacial periods of the Quaternary, their influence on long-term southern African climate change has been a matter of debate (e.g. Chase et al., 2019b; Collins et al., 2014; Dupont et al., 2011; Partridge et al., 1997; Stuut et al., 2002).

The discussion of the role of orbital forcing on southern African climates has often been structured in terms of remote (high latitude) versus direct (low latitude) mechanisms (Partridge et al., 1997; Thomas and Shaw, 2002; van Zinderen Bakker, 1976). High latitude mechanisms relate to the development of high latitude ice sheets and the impact of their expansion and contraction (including ice-rafting and meltwater pulses) on global atmospheric and oceanic circulation dynamics (Chase et al., 2015; Chevalier and Chase, 2015; Otto-Bliesner et al., 2014; Schefuß et al., 2011; Stuut and Lamy, 2004; Stuut et al., 2002; van Zinderen Bakker, 1967). Consideration of low latitude forcing generally relates to precession-driven changes in insolation seasonality, and their quasi-direct impact on regional and local precipitation through their influence on the development of convective and monsoonal systems (Kutzbach, 1981; Kutzbach et al., 2020; Partridge et al., 1997; Rossignol-Strick, 1983; Ruddiman, 2006b; Street-Perrott et al., 1990).

In southern Africa, high latitude forcing underpins the broadest conceptual models (Cockcroft et al., 1987; van Zinderen Bakker, 1976) and is also considered to be a significant factor in driving some abrupt climate change events (e.g. those associated with Heinrich stadial 1 and the Younger Dryas) (Chase et al., 2015; Chase et al., 2011; Schefuß et al., 2011). Broadly, these changes are related to global temperature variability, Northern Hemisphere ice-sheet development and dynamics, and Antarctic sea-ice extent. Global cooling – initiated by declining high latitude Northern Hemisphere summer insolation (Milankovitch, 1930), eccentricity (Broecker and van Donk, 1970; Hays et al., 1976) and the development of major ice-sheets (Ruddiman, 2006a) – is considered to have resulted in a decrease in rainfall in the SRZ through a reduction in evaporative and convective potential, and thus a reduction in the amount of moisture advection from adjacent oceans and the potential for precipitation events (Cockcroft et al., 1987; van Zinderen Bakker, 1976). In the WRZ, it is thought that this same cooling would have resulted in an expansion of Antarctic sea-ice, an expansion of the circum-polar vortex, and an equatorward shift of the storm tracks embedded in the southern westerlies, resulting in an increased occurrence of precipitation events in southwestern Africa (Cockcroft et al., 1987; Stuut et al., 2004; van Zinderen Bakker, 1976).

Considering southern Africa’s largely tropical-subtropical position, it is not surprising that an abundance of evidence exists indicating a strong influence of direct insolation forcing on regional climates. This evidence has been obtained from both terrestrial (Chase et al., 2019b; Partridge et al., 1997) and marine sediment records (Collins et al., 2014; Simon et al., 2015), and discussions primarily relate to variability in orbital precession (~23-kyr cycle) and changes in the range of the African tropical rainbelt (sometimes considered to be synonymous with the intertropical convergence zone (ITCZ)) tracking the zone of maximum summer insolation. While notable exceptions exist (e.g. southwestern Africa; Chase et al., 2019b), changes in hydroclimate associated with precessional forcing generally manifest as more (less) summer rainfall under higher (lower) summer insolation. Related to seasonal precipitation and insolation, these changes are thought to have been anti-phase between the Northern and Southern hemispheres (Kutzbach, 1981; Ruddiman, 2006b), but their strength in both hemispheres is directly related to changes in eccentricity, which determines the amount of insolation received. At high latitudes, eccentricity plays a role in determining the timing and duration of glacial cycles, particularly after mid-Pleistocene transition (MPT; ~1250 - 700 ka; Clark et al., 2006; Lisiecki and Raymo, 2005; Mudelsee and Schulz, 1997). It should be noted that this role is neither dominant nor isolated, as is sometimes assumed based on the similarity between the ~100-kyr eccentricity cycle and the average length of late Pleistocene glacial periods. Rather, eccentricity's influence is effected through its impact on precession, which works in concert with obliquity to establish the timing of glacial-interglacial cycles (Bajo et al., 2020; Huybers, 2006, 2011; Tzedakis et al., 2017). At low latitudes, eccentricity and precession have a more direct influence on climate, and, as will be shown, can be used as strong predictors of low latitude climate change over even longer timescales, extending back millions of years.

## Eccentricity

### *2400-kyr grand eccentricity cycle*

While precession is perhaps the most commonly considered parameter in southern Africa – as its strength and frequency make it most relevant to studies of late Quaternary low latitude climate change – changes in the precessional index are modulated by changes in eccentricity. Eccentricity varies at two primary periods relevant to Quaternary science, ~400-kyr and ~100-kyr, but longer "grand cycles" also exist, such as the 2400-kyr cycle (Boulila et al., 2012; Laskar et al., 2004; Olsen and Kent, 1996; Pälike et al., 2006a). While much weaker (Figure 2), these cycles have been highlighted as being significant environmental determinants over long, >$10^6$ $yr^{-1}$ timescales (Crampton et al., 2018; Pälike et al., 2006b). During the Quaternary Period, these cycles may also have had some influence, as there is a degree of consistency with long-term trends of Pleistocene hydroclimate in southeastern Africa. Records of terrestrial sediment flux in marine cores MD96-2048 (Caley et al., 2018) and IODP Site U1478 (Koutsodendris et al., 2021) off the Limpopo River mouth has been interpreted as reflecting regional rainfall variability, and from Lake Malawi a $\delta^{13}C$ record obtained from leaf waxes is interpreted as an indicator of vegetation and associated environmental change (Johnson et al., 2016). It should be noted that while complexities regarding the interpretation of the $\delta^{13}C_{wax}$ have been highlighted (Ivory et al., 2018), its coherent relationship with other hydroclimatic proxies from Lake Malawi (e.g. lake level; Lyons et al., 2015) is considered here to render it suitable for inclusion. At the scale of the 2400-kyr grand cycle in eccentricity, the MD96-2048 and U1478 records indicate patterns of variability prior to ~500-600 ka that would be consistent with a positive relationship between eccentricity and rainfall (Figure 3). At Lake Malawi, a similarly consistent, but opposite trend is observed, with increasingly humid conditions being inferred across the last million years (Johnson et al., 2016; Lyons et al., 2015). This spatio-temporal patterning of trends has been considered to indicate an equatorward shift of the southern limit of the African rainbelt (Caley et al., 2018), which is consistent with reconstructions of dynamics from more recent portions of the geological record (Chevalier and Chase, 2015). That this signal is not apparent in the LR04 global benthic foraminifera $\delta^{18}O$ record (Lisiecki and Raymo, 2005), which reflects changes in global ice volume, suggests that its influence may be restricted to lower latitudes. The marked deviation from the positive relationship between the 2400-kyr eccentricity cycle and terrestrial sediment flux in the Limpopo marine cores, particularly U1478, may relate to fundamental changes in global circulation systems after the MPT as a result of more extensive high latitude ice sheets and lower $CO_2$. It should be noted, however, that the chronology of the U1478 record is currently not based on based on an independent oxygen isotope stratigraphy, but employs the ln(Ti/Ca) record in an interpretive paradigm that presupposes a negative relationship between eccentricity and rainfall (Koutsodendris et al., 2021). The result differs notably from the chronology of the adjacent M96-2048, complicating consideration and comparison at this stage.

### *~400-kyr eccentricity cycle*

Considering that the ~400-kyr cycle is the strongest and most consistent of the eccentricity cycles (Figure 2), the expectation is that it will have been a significant determinant of long-term low latitude climate change, with increased tropical rainfall during periods of higher eccentricity. Across Africa, the response and interpretations of several long proxy records highlight different aspects of the environmental change related to eccentricity (Figure 4). The ODP 967 “wet/dry index” (Grant et al., 2017), for example, has been interpreted as having a strong relationship with hydroclimatic variability and exhibits a positive relationship with the ~400-kyr eccentricity cycle. In contrast, the dust flux records from ODP 659 (off West Africa; Tiedemann et al., 1994) and ODP 721/722 (off southeastern Arabia; deMenocal, 1995) have been interpreted in a way that indicates a negative relationship between humidity and the ~400-kyr eccentricity cycle (higher dust flux during periods of high eccentricity). The relationship between dust flux and climate is, however, likely more complex (cf. Trauth et al., 2009). One mechanism controlling variability in these records is almost certainly aridity, and the related erodibility of the landscape, as the original authors indicate. This aspect of environmental change likely explains the overall increase in dust flux to these sites across the Pleistocene, with the expansion of Northern Hemisphere ice sheets, the establishment of strong Walker circulation (Ravelo et al., 2004), and more significant arid periods in the Sahara. The positive correlation between eccentricity and records of both aridity (ODP 659 and ODP 721/722) and humidity (ODP 967, MD96-2048) at ~400-kyr frequencies, however, demands further consideration, particularly as sites such as Lake Magadi in Kenya (Owen et al., 2018) and Mukalla Cave (Nicholson et al., 2020), adjacent to ODP 721/722, indicate more humid conditions under high eccentricity at this frequency. Trauth et al. (2009) have suggested that dust fluxes at ODP 659 and ODP 721/722 may be significantly influenced by changes in monsoon circulation, with periods of high eccentricity resulting in increased aeolian sediment transport to the sites. It seems likely that the dust records are influenced by both direct insolation, particularly the ~400-kyr eccentricity cycle, and high-latitude forcing, which becomes a dominant control with the development of the ~100-kyr cycle after the onset of the MPT.

As with the 2400-kyr cycle, there are few records available from southern Africa that are long enough to be used to confirm and explore the influence of the ~400-kyr cycle. Again, MD96-2048 and Lake Malawi (Johnson et al., 2016; Lyons et al., 2015) have provided the best continuous records to date, and both express a ~400-kyr cycle of hydroclimatic variability (Figure 4). Similar to responses associated with the 2400-kyr cycle, the Lake Malawi lake level record (Lyons et al., 2015) exhibits a negative relationship with the ~400-kyr eccentricity cycle, while the MD96-2048 Fe/Ca terrestrial discharge record (Caley et al., 2018) correlates positively with eccentricity at this frequency, as does the lower resolution record of flowstone development from South Africa's Cradle of Humankind (Pickering et al., 2019) (Figure 4). It is interesting to note that while the strength of the ~400-kyr signal in the Lake Malawi record increases over the last 1300 kyr, it diminishes in the MD96-2048 Fe/Ca record. This also broadly coincides with the MPT and the change in dominance from ~41-kyr to ~100-kyr cycles in the LR04 global benthic foraminifera $\delta^{18}O$ record (Lisiecki and Raymo, 2005) and significant Northern Hemisphere ice sheet expansion. As with the circulation dynamics relating to the establishment of wetter conditions in the Zambezi region while regions to the north and south become more arid seems linked to Northern Hemisphere cooling (Chevalier and Chase, 2015; Schefuß et al., 2011; Wang et al., 2013), it may be that this trend is associated with the post-MPT development of high latitude ice sheets and perhaps the related development of a more strongly positive Indian Ocean Dipole (Johnson et al., 2016; Taylor et al., in press; Wang et al., 2015). The concurrent decrease in the ~400-kyr signal in the MD96-2048 Fe/Ca record may be a corollary of this same reorganisation of atmospheric and oceanic circulation systems influencing the region, also reflecting a shift from low-latitude forcing dominance in southern Africa to a scenario in which high-latitude forcing plays a more significant role.

In southwestern Africa, sea-surface temperature records (SSTs) from the ODP175-1082 (Etourneau et al., 2009) and ODP175-1084 marine cores (Marlow et al., 2000) from the Benguela Upwelling System (Figure 1) spanning the last 4600-kyr do not exhibit a strong ~400-kyr cyclicity consistent with eccentricity. This is similar to the response of the LR04 $\delta^{18}O$ record (Lisiecki and Raymo, 2005), which also exhibits extremely limited variability at this frequency (although the LR04 curve does express a generally negative relationship with eccentricity at this frequency prior to the MPT). The ODP 1082 and 1084 records, however, do show strong similarities with the LR04 record, both in its overall Plio-Pleistocene pattern (decreasing SSTs with increase global ice volume), and the development of an increasingly clear ~100-kyr cycle following the MPT (Figure 6).

### *~100-kyr cycles*

Following the MPT, c. 1250-700 ka, a ~100-kyr glacial-interglacial cycle became a much more significant aspect of global climate change (Clark et al., 2006; Lisiecki and Raymo, 2005; Mudelsee and Schulz, 1997). The drivers of this cycle remain a topic of active inquiry (e.g. Bajo et al., 2020), as the inception of prominent interglacial periods are not thought to be determined by the ~100-kyr eccentricity cycle per se - as may be inferred - but by the combined influence of precession and obliquity, with glacial periods of the late Pleistocene typically lasting two or three obliquity cycles (80 and 120 years, resulting in an average ~100-kyr periodicity) (Huybers, 2006, 2011; Tzedakis et al., 2017). This does not, however, mean the ~100-kyr eccentricity cycle has no influence, as it modulates the precessional cycle and is thus a significant factor in determining when insolation thresholds are crossed. In southern Africa, the source of the ~100-kyr cyclicities observed in fossil records depends on whether high or low latitude drivers are the dominant controls of regional climate dynamics. In regions dominated by high latitude drivers, changes observed at this wavelength are most likely attributable to the influence of obliquity and precession at high northern latitudes and the development of associated ice sheets. In tropical regions, particularly during periods of Earth's history when significant high latitude ice sheets were not present, variability at ~100-kyr cyclicities may more likely be driven by changes in direct insolation as modulated by eccentricity.

The importance of ~100-kyr cycles is evident in only some of the southeastern African records that extend back over multiple cycles. For example, the MD96-2048 Fe/Ca (Caley et al., 2018) and leaf wax $\delta^{13}C$ records (Castañeda et al., 2016) suggest phases of increased humidity that correlate well with higher eccentricity. Other records, such as those from Lake Malawi are more ambiguous, with a ~100-kyr cycle being only weakly expressed (Johnson et al., 2016; Lyons et al., 2015), and the Fe/K record from marine core CD154-10-06P (Simon et al., 2015) indicates – if anything – an opposing response. These differences may relate to changes in spatial climate response gradients during the Pleistocene, complex responses to the influences of high and low latitude forcing mechanisms, or limitations imposed by the chronologies of some sites. Establishing coherent scenarios that adequately explain the spatio-temporal variability observed across the region remains an area of active research.

As mentioned above, southeast Atlantic SSTs (Etourneau et al., 2009; Marlow et al., 2000) exhibit a strong positive correlation with the LR04 benthic $\delta^{18}O$ record (Lisiecki and Raymo, 2005), including ~100-kyr cycles, indicating a strong high latitude influence. Dust records from adjacent marine cores MD96-2094 (Stuut et al., 2002) and MD96-2087 (Pichevin et al., 2005) indicate more aeolian sediment transport under stronger wind fields during glacial periods; linked with SSTs through upwelling and intensifications of the South Atlantic Anticyclone (Etourneau et al., 2009; Little et al., 1997; Marlow et al., 2000). The dust records have been employed to infer environmental conditions in southwestern Africa, with greater proportions of fine sediments being interpreted as indicating increased fluvial activity and increased humidity (Stuut et al., 2002). This interpretation demonstrates – as with the SST records – a strong correlation with the LR04 record, suggesting that cooler global conditions and more extensive polar ice sheets result in more humid conditions in the region. At these timescales, and comparing glacial versus interglacial conditions, terrestrial records from the region (Chase et al., 2019b; Lim et al., 2016; Scott et al., 2004), support these inferences, indicating that the last glacial period was generally more humid than the Holocene, with changes in potential evapotranspiration playing a significant role in determining regional water balance (with cooler periods being generally more humid; Chase et al., 2019b; Lim et al., 2016). However, the available data do highlight significant contradictions between marine and terrestrial records (a topic that will be discussed in greater detail in the section addressing ~23-kyr cycles) and care should be taken in applying these findings to shorter timescales.

In terms of accurately attributing the source of a ~100-kyr signal to low or high latitude mechanisms, the presence of a ~400-kyr signal and/or the dominance of a ~23-kyr signal that is consistent with direct insolation (e.g. the Botuverá Cave speleothem record from Brazil (Cruz Jr. et al., 2005)), may provide indications of low latitude forcing dominance. Where these signals are absent or strongly muted, and a significant ~41-kyr signal is observed, high latitude mechanisms may more likely be the source of the ~100-kyr cycle.

### *~41-kyr obliquity cycle*

Obliquity (axial tilt) modulates the intensity of seasonality, and primarily affects higher latitudes. As such – coupled with the length of the cycles in relation to the majority of available records – it is not surprising that it has not often been identified as a prominent signal in southern African records. In those records where a ~41-kyr cycle can be identified, its origin has been associated with changes in high northern latitude insolation and the related evolution of continental ice sheets. It may be important to note, however, that in idealised modelling experiments it has been found that obliquity-induced changes can be observed at low latitudes without changes in high latitude ice sheets (Bosmans et al., 2015). Under high obliquity scenarios, increased cross-equatorial insolation and temperature gradients draw increased moisture into the summer hemisphere, resulting in increased tropical precipitation both north and south of the equator. The influence of this low latitude response remains to be fully resolved, but it may have played a role in driving low latitude climate variability, particularly during periods of low global ice volume.

In southwestern Africa, the ~41-kyr cycles that characterise changes in Plio-Pleistocene global ice volume prior to the MPT (Lisiecki and Raymo, 2005) were apparently more significant prior to ~2000 ka in SE Atlantic SST records (Etourneau et al., 2009). In southeastern Africa, interpretations of different records vary, perhaps at least in part as a function of their resolution. Caley et al. have determined that SST and sea-surface salinity records from marine core MD96-2048 exhibit significant ~41-kyr cycles (Caley et al., 2018; Caley et al., 2011), while records of changes in terrestrial environments from the same core (Fe/Ca; Caley et al., 2018) are rather dominated by ~100-kyr and ~23-kyr cycles, suggesting perhaps that precipitation in the region is linked to land-sea temperature contrasts, rather than directly to SSTs (Caley et al., 2018). In contrast, the Plio-Pleistocene records from the adjacent marine core ODP U1478 (Figure 1) reflecting changes in the same catchment contains significant ~41-kyr cycles in both SSTs and leaf wax δD, suggesting that SSTs did have a direct influence on terrestrial climates, at least during the 4000-1800 ka interval (Taylor et al., in press).

Over the last ~200 kyr, the bulk $\delta^{13}C$ record from Lake Malawi (Lyons et al., 2015) contains a significant ~41-kyr cycle  as part of a pattern of variability that bears marked similarities to the glacial-interglacial periods registered in the LR04 benthic $\delta^{18}O$ record (Lisiecki and Raymo, 2005). Palaeovegetation records from marine core MD96-2048 (Castañeda et al., 2016; Dupont et al., 2011) also reveal changes similar to the glacial-interglacial cycles reflected in the LR04 record, but these patterns contrast with the MD96-2048 Fe/Ca record (Caley et al., 2018), perhaps indicating that vegetation change in the basin was more significantly influenced by temperature (Chevalier et al., 2020) or $CO_2$ (Dupont et al., 2019). At these shorter timescales, however, the MD96-2048 Fe/Ca record is also at odds with other regional records that have similarly been interpreted as reflecting changes in regional hydroclimates (Chevalier and Chase, 2015; Holmgren et al., 2003; Partridge et al., 1997), suggesting complexities in either the spatio-temporal patterning of climate anomalies or in the interpretation of the various proxies.

To further explore the nature of the response to changes in obliquity in SE Africa, semblance analysis (Cooper and Cowan, 2008) was used to analyse the relationship between terrestrial sediment flux from the Limpopo River (interpreted as a proxy for rainfall) and global ice volume. Employing, respectively, the MD96-2048 ln(Fe/Ca) record (Caley et al., 2018) and the LR04 benthic $\delta^{18}O$ record (Lisiecki and Raymo, 2005), and isolating the 41-kyr obliquity frequency, it can be observed that the correlation between terrestrial sediment flux and global ice volume associated with axial tilt has alternated between positive (more rainfall during glacial periods) and negative (less rainfall during glacial periods) states (Figure 7). Interestingly, considering the 400-kyr component of these results, a pattern of variability consistent with the expansion of continental ice sheets across the last 2140 kyr is apparent. Prior to the MPT, increased ice volume is generally negatively correlated with runoff from the Limpopo Basin. During this period, long-term shifts toward a more positive relationship between runoff and ice volume occur during phases of increased eccentricity, suggesting a dynamic of wetter conditions during higher obliquity with eccentricity acting as a significant modulator. This may indicate 1) a muting of tropical rainfall even during the weak pre-MPT glacial periods, and/or 2) a scenario in which increased obliquity affects regional climates through an increase in cross-equatorial temperature gradients and strengthened summer moisture transport (Bosmans et al., 2015), a dynamic that may be amplified under higher eccentricity and insolation. The MPT marks an important threshold in the relationship between orbital parameters, ice volume and SE African climate. During and after the MPT, the correlation between Limpopo River runoff and obliquity-induced changes in ice volume becomes more often positive, indicating increased runoff during phases of low obliquity. Significantly, this dynamic is most prevalent during periods of low eccentricity, when low latitude forcing is weakened, supporting the proposal that the relative strength of high and low latitude forcing mechanisms is critical for ascertaining the regional response to changes in orbital parameters (Chase et al., in press).

### *~23-kyr precessional cycles*

The ~23-kyr cycle of orbital precession is, by virtue of its relatively short length as well as southern Africa's generally low latitude position, the most widely recognised orbital cycle observed in the regional records available (e.g. Collins et al., 2014; Partridge et al., 1997; Simon et al., 2015). Its nature as a determinant of the seasonal distribution of solar insolation means that the cycle engenders an antiphase response between the Northern and Southern hemispheres, with phases of high boreal summer insolation also being phases of low austral summer insolation. As such, it has in some cases led to contradictory interpretations of whether high or low latitude forcing is responsible for a given ~23-kyr signal (cf. Collins et al., 2014; Stuut et al., 2002). In southwestern Africa, this can be conceptualised either as an expansion/intensification of tropical systems and increased summer rainfall under increased direct summer insolation (e.g. Collins et al., 2014), or, alternatively, as an expansion/shift of the southern westerlies and increase in winter rainfall during cooler conditions induced by reduced high latitude boreal summer insolation (e.g. Stuut et al., 2002). In southeastern Africa, this dichotomy can be considered in terms of push and pull factors, with the African tropical rainbelt either being displaced southward as a result of Northern Hemisphere cooling (e.g. Schefuß et al., 2011), or drawn southward as it tracks the zone of maximum summer insolation (e.g. Partridge et al., 1997).

In southern Africa, the influence of precessional forcing appears to be both temporally and spatially variable. In southeastern Africa, evidence from lacustrine sediments from Tswaing Crater (Partridge et al., 1997) and from the marine core CD154 10-06P Fe/K record (Simon et al., 2015) (Figure 1) both indicate a strong precessional signal. It should be noted that the Tswaing Crater record of Partridge et al. (1997) was, based on its dominant 23-kyr cycle, tuned slightly to precession to improve its chronology for the period between the oldest radiocarbon age and the basal fission track age estimate. While initially contentious, this tuning is now supported by records such as the CD154 10-06P Fe/K record (Simon et al., 2015) and speleothem records from southernmost Africa's Cape Fold Mountains (Braun et al., 2020; Chase et al., in press; Talma and Vogel, 1992). After approximately ~70 ka the relationship between precession and regional hydroclimates begins to break down (Figures 8 and 9), a dynamic that has been assessed and clarified by Chase et al. (in press) through comparisons with the RC09-166 leaf wax δD record from the northern tropics in the Gulf of Aden (Tierney et al., 2017) and Chinese speleothem composite $\delta^{18}O$ record (Cheng et al., 2016). Findings indicate that under high eccentricity during MIS 5 southeast African tropical rainfall increased during periods of high local insolation, antiphase to trends in the northern tropics and consistent with Kutzbach's orbital monsoon hypothesis (Kutzbach, 1981). However, at ~70 ka – broadly concurrent with the establishment of pan-Arctic ice sheets in MIS 4 (Batchelor et al., 2019) – rainfall variability in southeastern Africa adopts a signal that is in-phase with the northern tropics. This in-phase relationship persists until the onset of the Holocene, when high latitude ice sheets retreated and direct local insolation forcing once again became the dominant driver of southeast African rainfall variability (Chase et al., in press). Additionally, interpretation of the Cape Fold speleothem $\delta^{18}O$ record pre-dating the transition at ~70 ka is generally consistent with changes in rainfall amount associated with the "amount effect" (Dansgaard, 1964; Herrmann et al., 2017), consistent with an expanded summer rainfall zone. After ~70 ka, when an obliquity cycle becomes apparent, speleothem $\delta^{18}O$ likely reflects changes in regional temperatures, suggesting a change in rainfall regimes and a restriction of the zone of tropical dominance (Chase et al., in press).

Along the southeast African margin, displacements of the African rainbelt associated with high northern latitude forcing have been cited as a potential control on the spatio-temporal patterns of orbital and sub-orbital climate variability across the last 50 kyr (Chevalier and Chase, 2015). Records from eastern African lake sites such as Lake Tanganyika show clear affinities with high latitude Northern Hemisphere signals, particularly during MIS 2 and the end of MIS 3 (~10-30 ka), when cold conditions in the north, and particularly the North Atlantic basin, induce dry conditions at the site (Tierney et al., 2008). As with the regionally anti-phase response of the Lake Malawi basin at longer orbital timescales noted above, leaf wax δD records from marine cores GIK 16160-3 (Wang et al., 2013) and GeoB 9307-3 (Schefuß et al., 2011) reflecting changes in the Zambezi Basin indicate an opposing response, with the Last Glacial Maximum (LGM; 19-26.5 ka), Heinrich Stadial 1 (HS1; ~18-14.6 ka) and the Younger Dryas (12.9-11.7 ka) experiencing increased rainfall, as the African rainbelt was displaced to the south. To the south of the Zambezi, in South Africa, records indicate conditions similar to those at Lake Tanganyika, apparently constraining the zone of increased precipitation during periods of Northern Hemisphere cooling to a narrow band between ~15 and 20°S (Chevalier and Chase, 2015). As the high latitude ice sheets diminished, $CO_2$ increased and global temperatures warmed, direct precessional forcing once again became the dominant control on long-term climate change throughout eastern Africa (Chevalier and Chase, 2015).

These findings have important implications for the use of Earth system/general circulation models (ESMs/GCMs) to study past climate change dynamics in southern Africa. In these models, insolation is a dominant determinant of low latitude climate change, and as such simulations of palaeo-precipitation often exhibit patterns of variability consistent with precessional cycles (Gordon et al., 2000; Pope et al., 2000), including relatively wetter conditions across much of southern Africa during the LGM (Engelbrecht et al., 2019; Schmidt et al., 2014; Sueyoshi et al., 2013). Regional data-model comparisons, however, indicate that when direct insolation forcing is reduced during phases of low eccentricity other drivers may become more significant (Singarayer and Burrough, 2015), that ESM performance may be limited in the region (Chevalier et al., 2017) and that such simulations should only be employed with due caution.

It should be considered too in terms of low latitude forcing that phases of high eccentricity and strong precessional influence may experience much wetter conditions during summer insolation maxima, but they also appear – at least in some cases – to experience much drier periods during summer insolation minima, and long-term climatic variability tends to increase (Lyons et al., 2015; Scholz et al., 2007). Despite this increased variability, the MD96-2048 record (Caley et al., 2018), indicates increases in mean humidity consistent with ~2400-kyr, ~400-kyr and ~100-kyr eccentricity cycles, suggesting that at least in the Limpopo catchment, phases of high eccentricity are associated with higher humidity.

Considering the spatial variability of precessional signals, data from a series of rock hyrax middens from the Namib Desert region on the western margin of southern Africa provide evidence of the influence of precession over the last 50 kyr. In this region, periods of high summer insolation are characterised by increased aridity (Chase et al., 2019b). This reflects the combined influence of higher low latitude insolation reducing atmospheric pressure over the continent, with concomitant high latitude cooling and steeper hemispheric temperature gradients resulting in intensifications of the South Atlantic Anticyclone. The increased land-sea pressure gradient led to the advection of cold air off the SE Atlantic, and drier conditions in the Namib Desert. These findings do raise questions about the inferences made regarding marine records recovered offshore from Namibia, such as the MD08-3167 leaf wax δD record, which indicates a positive relationship between precipitation and summer insolation (Collins et al., 2014). One possibility indicated by the authors is that the source of the sediment fractions analysed for this record lies to the north or east of the Namib Desert. The persistence of the precessional signal from 10-70 ka (Figure 10) suggests that the source area is not as far east as Tswaing Crater. However, the Makgadikgadi basin of the middle Kalahari is a major dust source (Vickery et al., 2013), and the MD08-3167 data may thus reflect conditions in this region. This spatial heterogeneity of signals may also relate to past dynamics of the Congo Air Boundary, which is defined by the boundary between Atlantic and Indian ocean air masses, and is associated with the southern margin of the African rainbelt in southwestern Africa (Howard and Washington, 2019), and has been invoked as a possible explanation for some aspects of palaeoclimatic variability in the Makgadikgadi region (Cordova et al., 2017). It should be noted, however, that the few records available from this region appear to indicate relatively humid Holocene conditions (Burrough et al., 2009; Burrough et al., 2007; Cordova et al., 2017). While consistent with a precessional driver, these findings contrast with the MD08-3167 data, which exhibits a markedly drier Holocene (Collins et al., 2014).

Another possibility is that rather than relating to changes in terrestrial environments, the marine core records of the southeast Atlantic are strongly influenced by changes in terrigenous sediment source region related to the strength and position of the southeast trade winds and the descending limb of the South Atlantic Anticyclone (Figure 11). This is suggested by the periodic inclusion of significant percentages of Restionaceae pollen (Cape reeds) in the region's marine sediments (Shi et al., 2001), despite no concurrent changes in this taxon being found at terrestrial sites from the Namib or Kalahari regions (Cordova et al., 2017; Lim et al., 2016; Scott et al., 2004). Variability of this wind field maintains a strong precessional signal throughout the last glacial period, driven as it is in part by changes in inter- and intra-hemispheric temperature gradients that are most pronounced during glacial periods and most particularly phases of pronounced high-latitude cooling associated with decreased boreal summer insolation (Figure 11). As such, it may be that the MD08-3167 δD record primarily reflects changes in the extent and position of the source region, with sediment being primarily derived from the arid Namib region during periods of reduced wind strength, and from more humid regions to the south when the wind field was stronger and more extensive. This scenario - which could also determine the variability observed in other marine records from the Southeast Atlantic - would provide a more comprehensive explanation for the variability observed in the MD08-3167 record, including the long-term decrease in δD values across the last glacial period and the relatively high values during the Holocene (Figure 11), but the resolution of these questions remains a matter for discussion and comparison with a fuller continental dataset.

## Inferences of climate variability in southern Africa based on orbital forcing

Establishing a framework of climate change dynamics and environmental change in southern Africa is, as mentioned, problematic, as so little evidence is available from the region. This paper establishes in general terms, based on the records available, the climatic response to changes in earth's orbital parameters with the goal of informing inferences of environmental change for periods and regions where direct proxy evidence is not available.

At the broadest scale, it appears likely that southwestern and southeastern Africa have, despite the same latitude, experienced markedly different environmental histories, and generally respond to fundamentally different drivers. In southwestern Africa, SST records from SE Atlantic marine cores (Etourneau et al., 2009; Marlow et al., 2000) closely mirror the variability observed in the LR04 global benthic foraminifera $\delta^{18}O$ record (Lisiecki and Raymo, 2005), indicating that variability in this system is closely tied to the development of high latitude ice sheets. A variety of proxy records obtained from SE Atlantic marine cores spanning the last glacial-interglacial cycle have been interpreted as indicating windier conditions associated with an intensified/displaced South Atlantic anticyclone during phases of global cooling (Little et al., 1997; Pichevin et al., 2005; Stuut et al., 2002), coupled with increased winter rainfall (Shi et al., 2001) and more humid conditions in southwestern Africa (Stuut et al., 2004; Stuut et al., 2002). While the wind field and upwelling reconstructions appear robust, inferences of changes in terrestrial environments have been shown to be more complicated, with significant contradictions existing between marine (Collins et al., 2014; Shi et al., 2001) and terrestrial records (Chase et al., 2019b; Lim et al., 2016; Scott et al., 2004). The best resolved terrestrial records indicate that the last glacial period was generally more humid than the Holocene, but that periods of increased upwelling – concurrent with lower boreal summer insolation – were relatively arid, driven by the advection of cool, dry air from the Atlantic margin (Chase et al., 2019b). This suggests that while changes in potential evapotranspiration play a significant role in determining regional water balance (with cooler periods being generally more humid; Chase et al., 2019b; Lim et al., 2016), precipitation exhibits a positive relationship with Benguela SSTs (Chase et al., 2015; Chase et al., 2019b). This information can be applied to the SE Atlantic SST records to infer general patterns of terrestrial environmental change along the western continental margin.

In southeastern Africa, at orbital timescales, precipitation variability is most clearly controlled by changes in eccentricity and precession as they influence the amount and seasonality of direct insolation. Significant correlations exist between proxy precipitation records and ~100-kyr, ~400-kyr and perhaps even ~2400-kyr cycles of eccentricity (Caley et al., 2018; Johnson et al., 2016; Lyons et al., 2015). This recognition sheds light on some previously confounding patterns, such as contextualising the age distributions of the Cradle of Humankind flowstones, which the authors concluded could not be easily explained by changes in insolation (Pickering et al., 2019). As described above, the Lake Malawi region and Zambezi basin present an intriguing anomaly along an otherwise relatively homogeneous climate response gradient spanning much of Africa's eastern margin (Chevalier and Chase, 2015; Johnson et al., 2016; Schefuß et al., 2011; Wang et al., 2013). With this exception, increased eccentricity generally results in increased rainfall/more humid conditions in the eastern tropics. This relationship, however, apparently weakens during periods of reduced eccentricity and higher global ice volume.

Based on these records and results, it may be suggested as a general guideline that under low eccentricity (<~0.035) and high global ice volume (LR04 $\delta^{18}O$ values >~4.3‰), the influence of direct forcing will decline and high latitude forcing may become more significant in the region (e.g. Figure 7). As discussed above, the impact of this increased influence of high latitude forcing is apparent in the breakdown of the positive relationship generally observed between precipitation and local summer insolation at ~23-kyr precessional cycles (Chase et al., in press; Chevalier and Chase, 2015; Partridge et al., 1997). These periods may have only occurred during the more intense glacial periods of the last ~700-kyr, but precise thresholds are difficult to establish, as the available proxy records and associated chronologies do not currently enable such exact refinement. These guideline values might, however, serve as an indicator for when climate predictions based on local insolation values alone may become less reliable.

The relationships and basic models described here have been defined using data obtained primarily from the continental margins. While Lake Malawi and Tswaing Crater are located further inland (~600 km and ~500 km respectively), no suitably resolved long records exist from the continental interior (see Chase and Meadows, 2007; Singarayer and Burrough, 2015; Thomas and Burrough, 2012). Records such as the MD08-3167 δD record (Collins et al., 2014) have been suggested to reflect conditions closer to the interior, but its spatial and environmental significance has yet to be fully resolved (Chase et al., 2019b; Collins et al., 2014; Singarayer and Burrough, 2015).

Over shorter timescales, considering finer-scale cycles and events, the relationships described here become – or are apparently – more complex. It is clear that the available data pose many questions that remain to be answered regarding the spatio-temporal nature of the observed anomalies and their significance in the context of changes in the global climate system. It is concluded though that the coupled consideration of orbital parameters and global boundary conditions and climate state provides a useful – if general – indication of the potential of southern Africa's diverse atmospheric and oceanic circulation systems to influence regional environments. This may serve as a basis for both refining ideas regarding the evolution of the region's biodiversity and human history and enabling more rigorous hypothesis testing for the role of climate variability as a driver of these processes.


## Acknowledgements

I thank Tom Johnson, Andrew Carr, Lynne Quick, Manuel Chevalier, Martin Trauth, and three anonymous reviewers for the constructive comments, input and perspective that have helped improve this contribution. I also thank all of the researchers who have worked so hard to produce the datasets and ideas considered in this paper.


## References


Bajo, P., Drysdale, R.N., Woodhead, J.D., Hellstrom, J.C., Hodell, D., Ferretti, P., Voelker, A.H.L., Zanchetta, G., Rodrigues, T., Wolff, E., Tyler, J., Frisia, S., Spötl, C., Fallick, A.E., 2020. Persistent influence of obliquity on ice age terminations since the Middle Pleistocene transition. Science 367, 1235-1239.

Batchelor, C.L., Margold, M., Krapp, M., Murton, D.K., Dalton, A.S., Gibbard, P.L., Stokes, C.R., Murton, J.B., Manica, A., 2019. The configuration of Northern Hemisphere ice sheets through the Quaternary. Nature Communications 10, 3713.

Berger, A., Imbrie, J., Hays, J., Kukla, G., Saltzman, B., 1984. Milankovitch and Climate.

Bosmans, J.H.C., Hilgen, F.J., Tuenter, E., Lourens, L.J., 2015. Obliquity forcing of low-latitude climate. Clim. Past 11, 1335-1346.

Boulila, S., Galbrun, B., Laskar, J., Pälike, H., 2012. A ~9myr cycle in Cenozoic $\delta^{13}$C record and long-term orbital eccentricity modulation: Is there a link? Earth and Planetary Science Letters 317-318, 273-281.
Braun, K., Bar-Matthews, M., Matthews, A., Ayalon, A., Cowling, R.M., Karkanas, P., Fisher, E.C., Dyez, K., Zilberman, T., Marean, C.W., 2019. Late Pleistocene records of speleothem stable isotopic compositions from Pinnacle Point on the South African south coast. Quaternary Research 91, 265-288.
Braun, K., Bar-Matthews, M., Matthews, A., Ayalon, A., Zilberman, T., Cowling, R.M., Fisher, E.C., Herries, A.I.R., Brink, J.S., Marean, C.W., 2020. Comparison of climate and environment on the edge of the Palaeo-Agulhas Plain to the Little Karoo (South Africa) in Marine Isotope Stages 5–3 as indicated by speleothems. Quaternary Science Reviews 235, 105803.
Broecker, W.S., van Donk, J., 1970. Insolation changes, ice volumes, and the $O^{18}$ record in deep-sea cores. Reviews of Geophysics 8, 169-198.
Burrough, S.L., Thomas, D.S.G., Bailey, R.M., 2009. Mega-Lake in the Kalahari: a late Pleistocene record of the Palaeolake Makgadikgadi system. Quaternary Science Reviews 28, 1392-1411.
Burrough, S.L., Thomas, D.S.G., Shaw, P.A., Bailey, R.M., 2007. Multiphase Quaternary highstands at Lake Ngami, Kalahari, northern Botswana. Palaeogeography, Palaeoclimatology, Palaeoecology 253, 280-299.
Caley, T., Extier, T., Collins, J.A., Schefuß, E., Dupont, L., Malaizé, B., Rossignol, L., Souron, A., McClymont, E.L., Jimenez-Espejo, F.J., García-Comas, C., Eynaud, F., Martinez, P., Roche, D.M., Jorry, S.J., Charlier, K., Wary, M., Gourves, P.-Y., Billy, I., Giraudeau, J., 2018. A two-million-year-long hydroclimatic context for hominin evolution in southeastern Africa. Nature 560, 76-79.
Caley, T., Kim, J.H., Malaizé, B., Giraudeau, J., Laepple, T., Caillon, N., Charlier, K., Rebaubier, H., Rossignol, L., Castañeda, I.S., Schouten, S., Sinninghe Damsté, J.S., 2011. High-latitude obliquity as a dominant forcing in the Agulhas current system. Climates of the Past 7, 1285-1296.
Castañeda, I.S., Caley, T., Dupont, L., Kim, J.-H., Malaizé, B., Schouten, S., 2016. Middle to Late Pleistocene vegetation and climate change in subtropical southern East Africa. Earth and Planetary Science Letters 450, 306-316.
Chappell, J., 1973. Astronomical theory of climatic change: status and problem. Quaternary Research 3, 221-236.
Chase, B., Harris, C., Wit, M.J.d., Kramers, J., Doel, S., Stankiewicz, J., in press. South African speleothems reveal influence of high- and low latitude forcing over the last 113.5 kyr. Geology.
Chase, B.M., Boom, A., Carr, A.S., Carré, M., Chevalier, M., Meadows, M.E., Pedro, J.B., Stager, J.C., Reimer, P.J., 2015. Evolving southwest African response to abrupt deglacial North Atlantic climate change events. Quaternary Science Reviews 121, 132-136.
Chase, B.M., Boom, A., Carr, A.S., Chevalier, M., Quick, L.J., Verboom, G.A., Reimer, P.J., 2019a. Extreme hydroclimate response gradients within the western Cape Floristic region of South Africa since the Last Glacial Maximum. Quaternary Science Reviews 219, 297-307.
Chase, B.M., Chevalier, M., Boom, A., Carr, A.S., 2017. The dynamic relationship between temperate and tropical circulation systems across South Africa since the last glacial maximum. Quaternary Science Reviews 174, 54-62.
Chase, B.M., Meadows, M.E., 2007. Late Quaternary dynamics of southern Africa's winter rainfall zone. Earth-Science Reviews 84, 103-138.
Chase, B.M., Niedermeyer, E.M., Boom, A., Carr, A.S., Chevalier, M., He, F., Meadows, M.E., Ogle, N., Reimer, P.J., 2019b. Orbital controls on Namib Desert hydroclimate over the past 50,000 years. Geology.
Chase, B.M., Quick, L.J., 2018. Influence of Agulhas forcing of Holocene climate change in South Africa's southern Cape. Quaternary Research 90, 303-309.
Chase, B.M., Quick, L.J., Meadows, M.E., Scott, L., Thomas, D.S.G., Reimer, P.J., 2011. Late glacial interhemispheric climate dynamics revealed in South African hyrax middens. Geology 39, 19-22.

Cheng, H., Edwards, R.L., Sinha, A., Spötl, C., Yi, L., Chen, S., Kelly, M., Kathayat, G., Wang, X., Li, X., Kong, X., Wang, Y., Ning, Y., Zhang, H., 2016. The Asian monsoon over the past 640,000 years and ice age terminations. Nature 534, 640.

Chevalier, M., Brewer, S., Chase, B.M., 2017. Qualitative assessment of PMIP3 rainfall simulations across the eastern African monsoon domains during the mid-Holocene and the Last Glacial Maximum. Quaternary Science Reviews 156, 107--120.

Chevalier, M., Chase, B.M., 2015. Southeast African records reveal a coherent shift from high- to low-latitude forcing mechanisms along the east African margin across last glacial–interglacial transition. Quaternary Science Reviews 125, 117-130.

Chevalier, M., Chase, B.M., Quick, L.J., Dupont, L.M., Johnson, T.C., 2020. Temperature change in subtropical southeastern Africa during the past 790,000 yr. Geology.

Clark, P.U., Archer, D., Pollard, D., Blum, J.D., Rial, J.A., Brovkin, V., Mix, A.C., Pisias, N.G., Roy, M., 2006. The middle Pleistocene transition: characteristics, mechanisms, and implications for long-term changes in atmospheric $pCO_2$. Quaternary Science Reviews 25, 3150-3184.

Cockcroft, M.J., Wilkinson, M.J., Tyson, P.D., 1987. The application of a present-day climatic model to the late Quaternary in southern Africa. Climatic Change 10, 161-181.

Collins, J.A., Schefuß, E., Govin, A., Mulitza, S., Tiedemann, R., 2014. Insolation and glacial–interglacial control on southwestern African hydroclimate over the past 140 000 years. Earth and Planetary Science Letters 398, 1-10.

Cooper, G.R.J., Cowan, D.R., 2008. Comparing time series using wavelet-based semblance analysis. Computers & Geosciences 34, 95-102.

Cordova, C.E., Scott, L., Chase, B.M., Chevalier, M., 2017. Late Pleistocene-Holocene vegetation and climate change in the Middle Kalahari, Lake Ngami, Botswana. Quaternary Science Reviews 171, 199-215.

Crampton, J.S., Meyers, S.R., Cooper, R.A., Sadler, P.M., Foote, M., Harte, D., 2018. Pacing of Paleozoic macroevolutionary rates by Milankovitch grand cycles. Proceedings of the National Academy of Sciences 115, 5686-5691.

Crétat, J., Pohl, B., Dieppois, B., Berthou, S., Pergaud, J., 2019. The Angola Low: relationship with southern African rainfall and ENSO. Climate Dynamics 52, 1783-1803.

Crétat, J., Richard, Y., Pohl, B., Rouault, M., Reason, C., Fauchereau, N., 2012. Recurrent daily rainfall patterns over South Africa and associated dynamics during the core of the austral summer. International Journal of Climatology 32, 261-273.

Cruz Jr., F.W., Burns, S.J., Vuille, M., Karmann, I., Viana Jr., O., Sharp, W.D., Cardoso, A.O., Silva Dias, P.L., Ferrari, J.A., 2005. Insolation-driven changes in atmospheric circulation over the past 116,000 years in subtropical Brazil. Nature 434, 63-66.

Dansgaard, W., 1964. Stable isotopes in precipitation. Tellus 16, 436-447.

de Boor, C., 2001. A practical guide to splines. Springer.

deMenocal, P.B., 1995. Plio-Pleistocene African climate. Science 270, 53-59.

Dupont, L.M., Caley, T., Castañeda, I.S., 2019. Effects of atmospheric CO2 variability of the past 800 kyr on the biomes of southeast Africa. Clim. Past 15, 1083-1097.

Dupont, L.M., Caley, T., Kim, J.H., Castañeda, I., Malaizé, B., Giraudeau, J., 2011. Glacial-interglacial vegetation dynamics in South Eastern Africa coupled to sea surface temperature variations in the Western Indian Ocean. Clim. Past 7, 1209-1224.

Dupont, L.M., Kuhlmann, H., 2017. Glacial-interglacial vegetation change in the Zambezi catchment. Quaternary Science Reviews 155, 127-135.

Engelbrecht, F.A., Marean, C.W., Cowling, R.M., Engelbrecht, C.J., Neumann, F.H., Scott, L., Nkoana, R., O'Neal, D., Fisher, E., Shook, E., Franklin, J., Thatcher, M., McGregor, J.L., Van der Merwe, J., Dedekind, Z., Difford, M., 2019. Downscaling Last Glacial Maximum climate over southern Africa. Quaternary Science Reviews 226, 105879.

Etourneau, J., Martinez, P., Blanz, T., Schneider, R., 2009. Pliocene-Pleistocene variability of upwelling activity, productivity, and nutrient cycling in the Benguela region. Geology 37, 871-874.

Farmer, E.C., deMenocal, P.B., Marchitto, T.M., 2005. Holocene and deglacial ocean temperature variability in the Benguela upwelling region: implications for low-latitude atmospheric circulation. Paleoceanography 20, doi:10.1029/2004PA001049.

Gordon, C., Cooper, C., Senior, C.A., Banks, H., Gregory, J.M., Johns, T.C., Mitchell, J.F.B., Wood, R.A., 2000. The simulation of SST, sea ice extents and ocean heat transports in a version of the Hadley Centre coupled model without flux adjustments. Climate Dynamics 16, 147-168.

Grant, K.M., Rohling, E.J., Westerhold, T., Zabel, M., Heslop, D., Konijnendijk, T., Lourens, L., 2017. A 3 million year index for North African humidity/aridity and the implication of potential pan-African Humid periods. Quaternary Science Reviews 171, 100-118.

Hays, J.D., Imbrie, J., Shackleton, N.J., 1976. Variations in the earth's orbit: pacemaker of the Ice Ages. Science 194, 1121-1132.

Herrmann, N., Boom, A., Carr, A.S., Chase, B.M., West, A.G., Zabel, M., Schefuß, E., 2017. Hydrogen isotope fractionation of leaf wax n-alkanes in southern African soils. Organic Geochemistry 109, 1-13.

Hijmans, R., Cameron, S.E., Parra, J.L., Jones, P.G., Jarvis, A., 2005. Very high resolution interpolated climate surfaces for global land areas. International Journal of Climatology 25, 1965-1978.

Holmgren, K., Lee-Thorp, J.A., Cooper, G.R.J., Lundblad, K., Partridge, T.C., Scott, L., Sithaldeen, R., Talma, A.S., Tyson, P.D., 2003. Persistent millennial-scale climatic variability over the past 25,000 years in Southern Africa. Quaternary Science Reviews 22, 2311-2326.

Howard, E., Washington, R., 2019. Drylines in Southern Africa: Rediscovering the Congo Air Boundary. Journal of Climate 32, 8223-8242.

Huybers, P., 2006. Early Pleistocene Glacial Cycles and the Integrated Summer Insolation Forcing. Science 313, 508-511.

Huybers, P., 2011. Combined obliquity and precession pacing of late Pleistocene deglaciations. Nature 480, 229-232.

Imbrie, J., 1982. Astronomical theory of the Pleistocene ice ages: a brief historical review. Icarus 50, 408-422.

Imbrie, J., Hays, J.D., Martinson, D.G., McIntyre, A., Mix, A.C., Morley, J.J., Pisias, N.G., Prell, W.L., Shackleton, N.J., 1984. The orbital theory of Pleistocene climate: support from a revised chronology of the marine $\delta^{18}$O record, in: Berger, A., Imbrie, J., Hays, J., Kukla, G., Saltzman, B. (Eds.), Milankovitch and Climate, Part 1. Reidel Publishing Co., Dordrecht, pp. 269-305.

Ivory, S.J., Lézine, A.-M., Vincens, A., Cohen, A.S., 2018. Waxing and waning of forests: Late Quaternary biogeography of southeast Africa. Global Change Biology 24, 2939-2951.

Johnson, T.C., Werne, J.P., Brown, E.T., Abbott, A., Berke, M., Steinman, B.A., Halbur, J., Contreras, S., Grosshuesch, S., Deino, A., Scholz, C.A., Lyons, R.P., Schouten, S., Damsté, J.S.S., 2016. A progressively wetter climate in southern East Africa over the past 1.3 million years. Nature 537, 220-224.

Koutsodendris, A., Nakajima, K., Kaboth-Bahr, S., Berke, M.A., Franzese, A.M., Hall, I.R., Hemming, S.R., Just, J., LeVay, L.J., Pross, J., Robinson, R., 2021. A Plio-Pleistocene (c. 0–4 Ma) cyclostratigraphy for IODP Site U1478 (Mozambique Channel, SW Indian Ocean): Exploring an offshore record of paleoclimate and ecosystem variability in SE Africa. Newsletters on Stratigraphy 54, 159-181.

Kutzbach, J.E., 1981. Monsoon climate of the early Holocene: climate experiment with the Earth's orbital parameters for 9000 years ago. Science 214, 59-61.

Kutzbach, J.E., Guan, J., He, F., Cohen, A.S., Orland, I.J., Chen, G., 2020. African climate response to orbital and glacial forcing in 140,000-y simulation with implications for early modern human environments. Proceedings of the National Academy of Sciences, 201917673.

Laskar, J., Robutel, P., Joutel, F., Gastineau, M., Correia, A.C.M., Levrard, B., 2004. A long-term numerical solution for the insolation quantities of the Earth. A&A 428, 261-285.

Lim, S., Chase, B.M., Chevalier, M., Reimer, P.J., 2016. 50,000 years of vegetation and climate change in the southern Namib Desert, Pella, South Africa. Palaeogeography, Palaeoclimatology, Palaeoecology 451, 197-209.

Lisiecki, L.E., Raymo, M.E., 2005. A Pliocene-Pleistocene stack of 57 globally distributed benthic $\delta^{18}$O records. Paleoceanography 20, PA1003.

Little, M.G., Schneider, R.R., Kroon, D., Price, B., Bickert, T., Wefer, G., 1997. Rapid palaeoceanographic changes in the Benguela Upwelling System for the last 160,000 years as indicated by abundances of planktonic foraminifera. Palaeogeography, Palaeoclimatology, Palaeoecology 130, 135-161.

Lyons, R.P., Scholz, C.A., Cohen, A.S., King, J.W., Brown, E.T., Ivory, S.J., Johnson, T.C., Deino, A.L., Reinthal, P.N., McGlue, M.M., Blome, M.W., 2015. Continuous 1.3-million-year record of East African hydroclimate, and implications for patterns of evolution and biodiversity. Proceedings of the National Academy of Sciences 112, 15568-15573.

Marlow, J.R., Lange, C.B., Wefer, G., Rosell-Mele, A., 2000. Upwelling intensification as part of the Pliocene-Pleistocene climate transition. Science 290, 2288-2291.

Milankovitch, M.K., 1930. Mathematische Klimalehre und Astronornische Theorie der Klirnaschwankungen. Gebruder Borntraeger, Berlin.

Mudelsee, M., Schulz, M., 1997. The Mid-Pleistocene climate transition: onset of 100 ka cycle lags ice volume build-up by 280 ka. Earth and Planetary Science Letters 151, 117-123.

Nicholson, S.E., Entekhabi, D., 1987. Rainfall variability in equatorial and southern Africa: relationships with sea surface temperatures along the southwestern coast of Africa. Journal of Climate and Applied Meteorology 26, 561-578.

Nicholson, S.L., Pike, A.W.G., Hosfield, R., Roberts, N., Sahy, D., Woodhead, J., Cheng, H., Edwards, R.L., Affolter, S., Leuenberger, M., Burns, S.J., Matter, A., Fleitmann, D., 2020. Pluvial periods in Southern Arabia over the last 1.1 million-years. Quaternary Science Reviews 229, 106112.

Olsen, P.E., Kent, D.V., 1996. Milankovitch climate forcing in the tropics of Pangaea during the Late Triassic. Palaeogeography, Palaeoclimatology, Palaeoecology 122, 1-26.

Otto-Bliesner, B.L., Russell, J.M., Clark, P.U., Liu, Z., Overpeck, J.T., Konecky, B., deMenocal, P., Nicholson, S.E., He, F., Lu, Z., 2014. Coherent changes of southeastern equatorial and northern African rainfall during the last deglaciation. Science 346, 1223-1227.

Owen, R.B., Muiruri, V.M., Lowenstein, T.K., Renaut, R.W., Rabideaux, N., Luo, S., Deino, A.L., Sier, M.J., Dupont-Nivet, G., McNulty, E.P., Leet, K., Cohen, A., Campisano, C., Deocampo, D., Shen, C.-C., Billingsley, A., Mbuthia, A., 2018. Progressive aridification in East Africa over the last half million years and implications for human evolution. Proceedings of the National Academy of Sciences 115, 11174-11179.

Pälike, H., Frazier, J., Zachos, J.C., 2006a. Extended orbitally forced palaeoclimatic records from the equatorial Atlantic Ceara Rise. Quaternary Science Reviews 25, 3138-3149.

Pälike, H., Norris, R.D., Herrle, J.O., Wilson, P.A., Coxall, H.K., Lear, C.H., Shackleton, N.J., Tripati, A.K., Wade, B.S., 2006b. The Heartbeat of the Oligocene Climate System. Science 314, 1894-1898.

Partridge, T.C., deMenocal, P.B., Lorentz, S.A., Paiker, M.J., Vogel, J.C., 1997. Orbital forcing of climate over South Africa: a 200,000-year rainfall record from the Pretoria Saltpan. Quaternary Science Reviews 16, 1125-1133.

Peel, M.C., Finlayson, B.L., McMahon, T.A., 2007. Updated world map of the Köppen-Geiger climate classification. Hydrol. Earth Syst. Sci. 11, 1633-1644.

Peeters, F.J.C., Acheson, R., Brummer, G.-J.A., de Ruijter, W.P.M., Schneider, R.R., Ganssen, G.M., Ufkes, E., Kroon, D., 2004. Vigorous exchange between the Indian and Atlantic oceans at the end of the past five glacial periods. Nature 430, 661-665.

Pichevin, L., Cremer, M., Giraudeau, J., Bertrand, P., 2005. A 190 kyr record of lithogenic grain-size on the Namibian slope: forging a tight link between past wind-strength and coastal upwelling dynamics. Marine Geology 218, 81-96.

Pickering, R., Herries, A.I.R., Woodhead, J.D., Hellstrom, J.C., Green, H.E., Paul, B., Ritzman, T., Strait, D.S., Schoville, B.J., Hancox, P.J., 2019. U–Pb-dated flowstones restrict South African early hominin record to dry climate phases. Nature 565, 226-229.

Pope, V.D., Gallani, M.L., Rowntree, P.R., Stratton, R.A., 2000. The impact of new physical parametrizations in the Hadley Centre climate model: HadAM3. Climate Dynamics 16, 123-146.

Ravelo, A.C., Andreasen, D.H., Lyle, M., Olivarez Lyle, A., Wara, M.W., 2004. Regional climate shifts caused by gradual global cooling in the Pliocene epoch. Nature 429, 263-267.

Reason, C.J.C., Rouault, M., Melice, J.L., Jagadheesha, D., 2002. Interannual winter rainfall variability in SW South Africa and large scale ocean–atmosphere interactions. Meteorology and Atmospheric Physics 80, 19-29.
Rossignol-Strick, M., 1983. African monsoon, an immediate climate response to orbital insolation. Nature 304, 46-49.
Rouault, M., Florenchie, P., Fauchereau, N., Reason, C.J.C., 2003. South East tropical Atlantic warm events and southern African rainfall. Geophysical Research Letters 30.
Rouault, M., White, S.A., Reason, C.J.C., Lutjeharms, J.R.E., Jobard, I., 2002. Ocean–Atmosphere Interaction in the Agulhas Current Region and a South African Extreme Weather Event. Weather & Forecasting 17, 655.
Ruddiman, W.F., 2006a. Orbital changes and climate. Quaternary Science Reviews 25, 3092-3112.
Ruddiman, W.F., 2006b. What is the timing of orbital-scale monsoon changes? Quaternary Science Reviews 25, 657-658.
Schefuß, E., Kuhlmann, H., Mollenhauer, G., Prange, M., Pätzold, J., 2011. Forcing of wet phases in southeast Africa over the past 17,000 years. Nature 480, 509-512.
Schmidt, G.A., Kelley, M., Nazarenko, L., Ruedy, R., Russell, G.L., Aleinov, I., Bauer, M., Bauer, S.E., Bhat, M.K., Bleck, R., Canuto, V., Chen, Y.-H., Cheng, Y., Clune, T.L., Del Genio, A., de Fainchtein, R., Faluvegi, G., Hansen, J.E., Healy, R.J., Kiang, N.Y., Koch, D., Lacis, A.A., LeGrande, A.N., Lerner, J., Lo, K.K., Matthews, E.E., Menon, S., Miller, R.L., Oinas, V., Oloso, A.O., Perlwitz, J.P., Puma, M.J., Putman, W.M., Rind, D., Romanou, A., Sato, M., Shindell, D.T., Sun, S., Syed, R.A., Tausnev, N., Tsigaridis, K., Unger, N., Voulgarakis, A., Yao, M.-S., Zhang, J., 2014. Configuration and assessment of the GISS ModelE2 contributions to the CMIP5 archive. Journal of Advances in Modeling Earth Systems 6, 141-184.
Scholz, C.A., Johnson, T.C., Cohen, A.S., King, J.W., Peck, J.A., Overpeck, J.T., Talbot, M.R., Brown, E.T., Kalindekafe, L., Amoako, P.Y.O., Lyons, R.P., Shanahan, T.M., Castaneda, I.S., Heil, C.W., Forman, S.L., McHargue, L.R., Beuning, K.R., Gomez, J., Pierson, J., 2007. East African megadroughts between 135 and 75 thousand years ago and bearing on early-modern human origins. Proceedings of the National Academy of Sciences 104, 16416-16421.
Scott, L., Marais, E., Brook, G.A., 2004. Fossil hyrax dung and evidence of Late Pleistocene and Holocene vegetation types in the Namib Desert. Journal of Quaternary Science 19, 829-832.
Shi, N., Schneider, R., Beug, H.-J., Dupont, L.M., 2001. Southeast trade wind variations during the last 135 kyr: evidence from pollen spectra in eastern South Atlantic sediments. Earth and Planetary Science Letters 187, 311-321.
Simon, M.H., Ziegler, M., Bosmans, J., Barker, S., Reason, C.J.C., Hall, I.R., 2015. Eastern South African hydroclimate over the past 270,000 years. Scientific Reports 5, 18153.
Singarayer, J.S., Burrough, S.L., 2015. Interhemispheric dynamics of the African rainbelt during the late Quaternary. Quaternary Science Reviews 124, 48-67.
Singarayer, J.S., Valdes, P.J., 2010. High-latitude climate sensitivity to ice-sheet forcing over the last 120kyr. Quaternary Science Reviews 29, 43-55.
Street-Perrott, F.A., Mitchell, J.F.B., Marchand, D.S., Brunner, J.S., 1990. Milankovitch and albedo forcing of the tropical monsoons: a comparison of geological evidence and numerical simulations for 9000 BP. Transactions - Royal Society of Edinburgh: Earth Sciences 81, 407-427.
Stuut, J.-B.W., Crosta, X., van der Borg, K., Schneider, R., 2004. Relationship between Antarctic sea ice and southwest African climate during the late Quaternary. Geology 32, 909-912.
Stuut, J.-B.W., Lamy, F., 2004. Climate variability at the southern boundaries of the Namib (southwestern Africa) and Atacama (northern Chile) coastal deserts during the last 120,000 yr. Quaternary Research 62, 301-309.
Stuut, J.-B.W., Prins, M.A., Schneider, R.R., Weltje, G.J., Jansen, J.H.F., Postma, G., 2002. A 300 kyr record of aridity and wind strength in southwestern Africa: inferences from grain-size distributions of sediments on Walvis Ridge, SE Atlantic. Marine Geology 180, 221-233.
Sueyoshi, T., Ohgaito, R., Yamamoto, A., Chikamoto, M.O., Hajima, T., Okajima, H., Yoshimori, M., Abe, M., O'Ishi, R., Saito, F., Watanabe, S., Kawamiya, M., Abe-Ouchi, A., 2013. Set-up of the PMIP3

paleoclimate experiments conducted using an Earth system model, MIROC-ESM. Geosci. Model Dev. 6, 819-836.

Talma, A.S., Vogel, J.C., 1992. Late Quaternary paleotemperatures derived from a speleothem from Cango Caves, Cape Province, South Africa. Quaternary Research 37, 203-213.

Taylor, A.K., Berke, M.A., Castañeda, I.S., Koutsodendris, A., Campos, H., Hall, I.R., Hemming, S.R., LeVay, L.J., Sierra, A.C., O'Connor, K., Scientists, t.E., in press. Plio-Pleistocene Continental Hydroclimate and Indian Ocean Sea Surface Temperatures at the Southeast African Margin. Paleoceanography and Paleoclimatology n/a, e2020PA004186.

Thomas, D.S.G., Burrough, S.L., 2012. Interpreting geoproxies of late Quaternary climate change in African drylands: implications for understanding environmental change and early human behaviour. Quaternary International 253, 5-17.

Thomas, D.S.G., Shaw, P.A., 2002. Late Quaternary environmental change in central southern Africa: new data, synthesis, issues and prospects. Quaternary Science Reviews 21, 783-797.

Tiedemann, R., Sarnthein, M., Shackleton, N.J., 1994. Astronomic timescale for the Pliocene Atlantic δ18O and dust flux records of Ocean Drilling Program Site 659. Paleoceanography 9, 619-638.

Tierney, J.E., deMenocal, P.B., Zander, P.D., 2017. A climatic context for the out-of-Africa migration. Geology 45, 1023-1026.

Tierney, J.E., Russell, J.M., Huang, Y., Sinninghe Damsté, J.S., Hopmans, E.C., Cohen, A.S., 2008. Northern Hemisphere controls on tropical southeast African climate during the past 60,000 years. Science 322, 252-255.

Trauth, M.H., Larrasoaña, J.C., Mudelsee, M., 2009. Trends, rhythms and events in Plio-Pleistocene African climate. Quaternary Science Reviews 28, 399-411.

Tyson, P.D., 1986. Climatic Change and Variability in Southern Africa. Oxford University Press, Cape Town.

Tyson, P.D., Preston-Whyte, R.A., 2000. The Weather and Climate of Southern Africa. Oxford University Press, Cape Town.

Tzedakis, P.C., Crucifix, M., Mitsui, T., Wolff, E.W., 2017. A simple rule to determine which insolation cycles lead to interglacials. Nature 542, 427-432.

van Zinderen Bakker, E.M., 1967. Upper Pleistocene stratigraphy and Holocene ecology on the basis of vegetation changes in Sub-Saharan Africa, in: Bishop, W.W., Clark, J.D. (Eds.), Background to Evolution in Africa. University of Chicago Press, Chicago, pp. 125-147.

van Zinderen Bakker, E.M., 1976. The evolution of late Quaternary paleoclimates of Southern Africa. Palaeoecology of Africa 9, 160-202.

Vickery, K.J., Eckardt, F.D., Bryant, R.G., 2013. A sub-basin scale dust plume source frequency inventory for southern Africa, 2005-2008. Geophysical Research Letters 40, 5274-5279.

Wang, B., Ding, Q., 2008. Global monsoon: dominant mode of annual variation in the tropics. Dynamics of Atmospheres and Oceans 44, 165-183.

Wang, Y., Jian, Z., Zhao, P., Chen, J., Xiao, D., 2015. Precessional forced evolution of the Indian Ocean Dipole. Journal of Geophysical Research: Oceans 120, 3747-3760.

Wang, Y.V., Larsen, T., Leduc, G., Andersen, N., Blanz, T., Schneider, R.R., 2013. What does leaf wax δD from a mixed C3/C4 vegetation region tell us? Geochimica et Cosmochimica Acta 111, 128-139.

## Figure captions

**Figure 1:** Map of southern Africa with primary atmospheric (white arrows) and oceanic circulation systems (blue arrows or cold currents, red arrows for warm currents) indicated. Terrestrial colour gradient indicates seasonal distribution of precipitation, with reds (blues) indicating a dominance of austral summer (winter) rainfall linked to tropical (temperate) moisture-bearing systems. Sites discussed are indicated by numbered dots as follows: **(1)** MD96-2094 (Stuut et al., 2002); **(2)** ODP

1082 (Etourneau et al., 2009); **(3)** MD08-3167 (Collins et al., 2014); **(4)** GeoB 1711-4 (Little et al., 1997; Shi et al., 2001) **(5)** MD96-2087 (Pichevin et al., 2005); **(6)** ODP 1084 (Marlow et al., 2000); **(7a-c)** Namib Desert rock hyrax middens (Chase et al., 2019b); **(8)** MD96-2081 (Peeters et al., 2004); **(9)** Pinnacle Point (Braun et al., 2019); **(10)** Cango and Efflux caves (Braun et al., 2020; Chase et al., in press; Talma and Vogel, 1992); **(11)** CD154-10-06P (Simon et al., 2015); **(12)** Cradle of Humankind; **(13)** Tswaing Crater (Partridge et al., 1997); **(14)** MD96-2048 (Braun et al., 2020; Caley et al., 2018; Caley et al., 2011; Castañeda et al., 2016; Dupont et al., 2011); **(15)** ODP U1478 (Taylor et al., in press); **(16)** GeoB 9311-1 (Dupont and Kuhlmann, 2017); **(17)** GeoB 9307-3 (Schefuß et al., 2011); **(18)** GIK 16160-3 (Wang et al., 2013); **(19)** Lake Malawi (Johnson et al., 2016; Lyons et al., 2015).

**Figure 2:** Power spectrum from continuous Morlet wavelet transform of 10 Myr orbital eccentricity data (Laskar et al., 2004). The cone of influence indicates the region beyond which there is potential for edge effects The colour gradient indicates wavelet power (red = stronger signal), and the position of ~100-kyr, ~400-kyr and ~2400-kyr eccentricity cycles are highlighted by white dashed lines.

**Figure 3:** The ~2400-kyr orbital eccentricity cycle and records interpreted as indicators environmental variability from Lake Malawi (Johnson et al., 2016) and marine cores MD96-2048 (Caley et al., 2018) and Site U1478 (Koutsodendris et al., 2021) as well as the LR04 global benthic $\delta^{18}O$ record (Lisiecki and Raymo, 2005). The proxy records were smoothed to distil comparable signals using smoothing splines according to the algorithm of de Boor (2001).

**Figure 4:** Comparison of real-value wavelet power spectra at 400-kyr periods from continuous Morlet wavelet transforms of: 1) orbital eccentricity data (Laskar et al., 2004), 2) ODP 721/722 dust flux data (deMenocal, 1995), 3) ODP 659 dust flux data (Tiedemann et al., 1994), 4) ODP 967 wet/dry index (Grant et al., 2017), 5) MD96-2048 ln(Fe/Ca) data (Caley et al., 2018), and 6) Lake Malawi (MAL05-1) lake level reconstruction (Lyons et al., 2015). The colour gradient indicates real-value wavelet power (red indicates large positive anomalies while blue indicates large negative anomalies). The timing of the derived 400-kyr cycles is normalised (standard score) and compared to assess their phasing. The ~400-kyr eccentricity cycle is compared to ages and probability density functions from the Cradle of Humankind (CoH) flowstones (Pickering et al., 2019). Map indicates location of sites considered, and in green the extent of the African tropical rainbelt (data from Hijmans et al., 2005; calculated according to Wang and Ding, 2008).

**Figure 5:** Semblance analysis (Cooper and Cowan, 2008) of Lake Malawi lake level data (Lyons et al., 2015) and MD96-2048 ln(Fe/Ca) data (Caley et al., 2018) with orbital eccentricity data (Laskar et al., 2004). Middle panes indicate real-value wavelet power of proxy records and eccentricity at ~400-kyr periods (red indicates large positive anomalies while blue indicates large negative anomalies). In the

lower semblance pane, red indicates a semblance of +1 (positive correlation), and blue indicates a semblance of −1 (negative correlation).

**Figure 6:** Comparison of the LR04 global benthic $\delta^{18}O$ record (Lisiecki and Raymo, 2005) with the ODP 1082 sea-surface temperature record from the Benguela upwelling system (Etourneau et al., 2009). Timing of the mid-Pleistocene transition (MPT; as per Clark et al., 2006) is indicated.

**Figure 7:** Comparison of 1) orbital eccentricity (orange lines; Laskar et al., 2004) with dashed line showing 400-kyr cycle, and 2) 41-kyr obliquity component from semblance analysis (blue lines and heat map, with 400-kyr filter depicted as dashed line; Cooper and Cowan, 2008) of the MD96-2048 ln(Fe/Ca) record, interpreted as reflecting changes in terrestrial sediment flux as a function of changes in rainfall amount in the Limpopo Basin (Caley et al., 2018) and the LR04 benthic $\delta^{18}O$ record reflecting changes in global ice volume (Lisiecki and Raymo, 2005). Semblance results (in heat map red=positive correlation and blue= negative correlation) indicate the response of Limpopo Basin to changes in global ice volume associated with variations in obliquity. Positive (negative) values indicate increased (decreased) sediment flux during phases of increased ice volume and decreased axial tilt. Prior to the mid-Pleistocene transition (MPT), a negative relationship generally exists between runoff and obliquity. Following the MPT, primarily during periods of low eccentricity and weakened low latitude forcing, runoff appears to increase during glacial periods.

**Figure 8:** Orbital eccentricity and austral summer (DJF) insolation at 25°S (Laskar et al., 2004), and comparisons of summer insolation variability with the Tswaing Crater precipitation reconstruction (Partridge et al., 1997) and the CD154 10-06P Fe/K record (Simon et al., 2015).

**Figure 9:** Semblance analysis (Cooper and Cowan, 2008) of austral summer (DJF) insolation at 25°S (Laskar et al., 2004), the Tswaing Crater precipitation reconstruction (Partridge et al., 1997) and the CD154 10-06P Fe/K record (Simon et al., 2015). Colour in upper panes indicate real-value signal power (red indicates large positive anomalies whereas blue indicates large negative anomalies), whereas in the lower semblance pane, red indicates a semblance of +1 (positive correlation), and blue indicates a semblance of −1 (negative correlation).

**Figure 10:** Comparison of austral summer (DJF) insolation at 25°S (Laskar et al., 2004), quasi-transient HadCM3 Earth system model simulation of mean annual precipitation at Tswaing Crater (Gordon et al., 2000; Pope et al., 2000; Singarayer and Valdes, 2010), and the Tswaing Crater precipitation reconstruction (Partridge et al., 1997). Heat map presents results of semblance analysis of HadCM3 and proxy-based precipitation reconstruction for Tswaing Crater (red=positive correlation and blue= negative correlation). Green shading indicates phases of above average summer insolation at Tswaing Crater. The dark blue line indicates the ~21 ka period used by the PMIP3 models, of which

the ensemble 21 ka – pre-industrial precipitation simulation is shown in the lower pane (from Chevalier et al., 2017). The location of Tswaing Crater is indicated by the orange dot. Inter-model agreement on the sign of the anomalies at ~75/90%, which correspond to an agreement of seven and eight out of the nine models, is indicated by red dots/crosses, respectively.

**Figure 11:** Comparison of LR04 benthic $\delta^{18}O$ stack (higher values indicate increased global ice volume; Lisiecki and Raymo, 2005), boreal summer (DJF) insolation at 60°N (Laskar et al., 2004), the leaf wax $\delta D$ record from marine core MD08-3167 (lower values indicate more humid conditions; Collins et al., 2014), and the composite record of SE Atlantic wind strength proxies (higher values indicate increased wind strength; Chase et al., 2019a; data from Farmer et al., 2005; Little et al., 1997; Pichevin et al., 2005; Stuut et al., 2002). Blue bars highlight periods of low boreal summer insolation at precessional wavelengths.

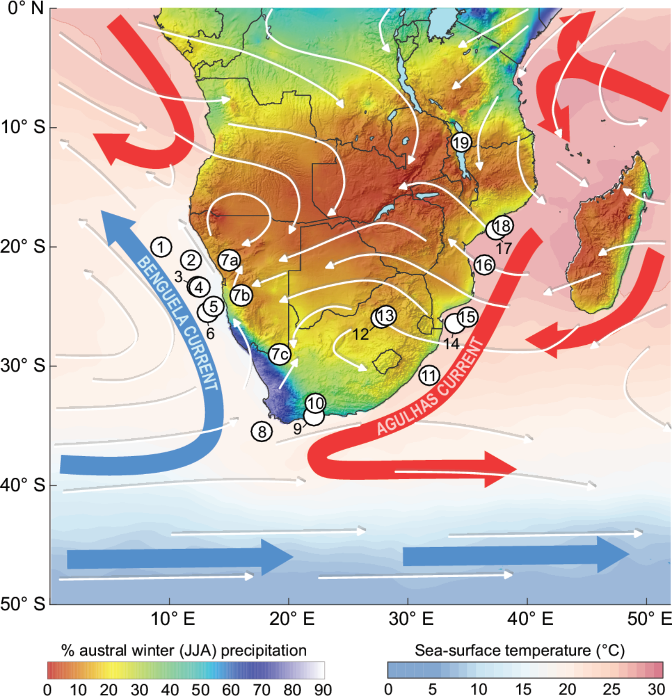

0° N
10° S
20° S
30° S
40° S
50° S
10° E
20° E
30° E
40° E
50° E
BENGUELA CURRENT
AGULHAS CURRENT
1
2
3
4
5
6
7a
7b
7c
8
9
10
11
12
13
14
15
16
17
18
19
% austral winter (JJA) precipitation
0 10 20 30 40 50 60 70 80 90
Sea-surface temperature (°C)
0 5 10 15 20 25 30

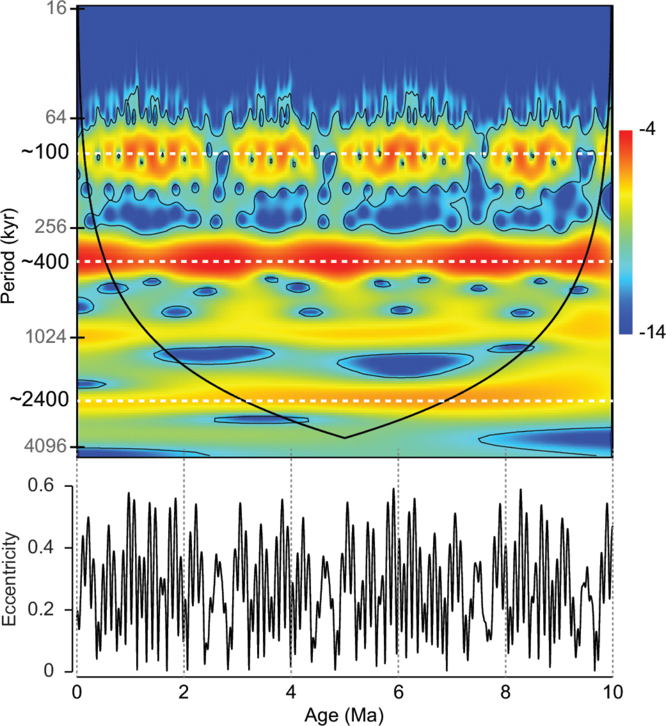

16
64
~100
256
~400
1024
~2400
4096
Period (kyr)
-4
-14
0.6
0.4
0.2
0
Eccentricity
0
2
4
6
8
10
Age (Ma)

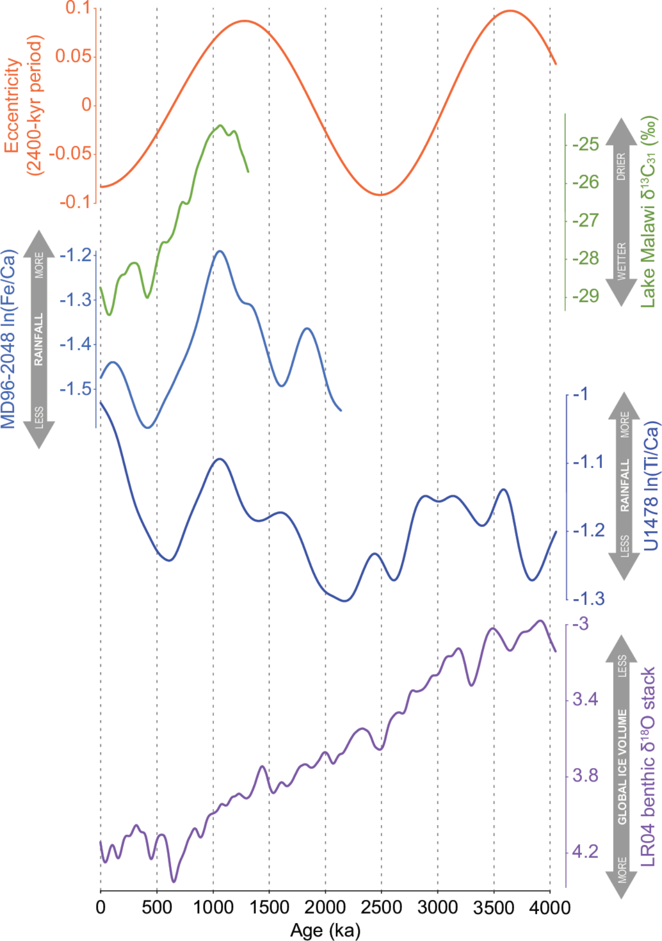

Eccentricity
(2400-kyr period)
0.1
0.05
0
-0.05
-0.1
Lake Malawi δ13C31 (‰)
-25
-26
-27
-28
-29
DRIER
WETTER
MD96-2048 ln(Fe/Ca)
-1.2
-1.3
-1.4
-1.5
MORE
RAINFALL
LESS
U1478 ln(Ti/Ca)
-1
-1.1
-1.2
-1.3
MORE
RAINFALL
LESS
LR04 benthic δ18O stack
-3
3.4
3.8
4.2
LESS
GLOBAL ICE VOLUME
MORE
0
500
1000
1500
2000
2500
3000
3500
4000
Age (ka)

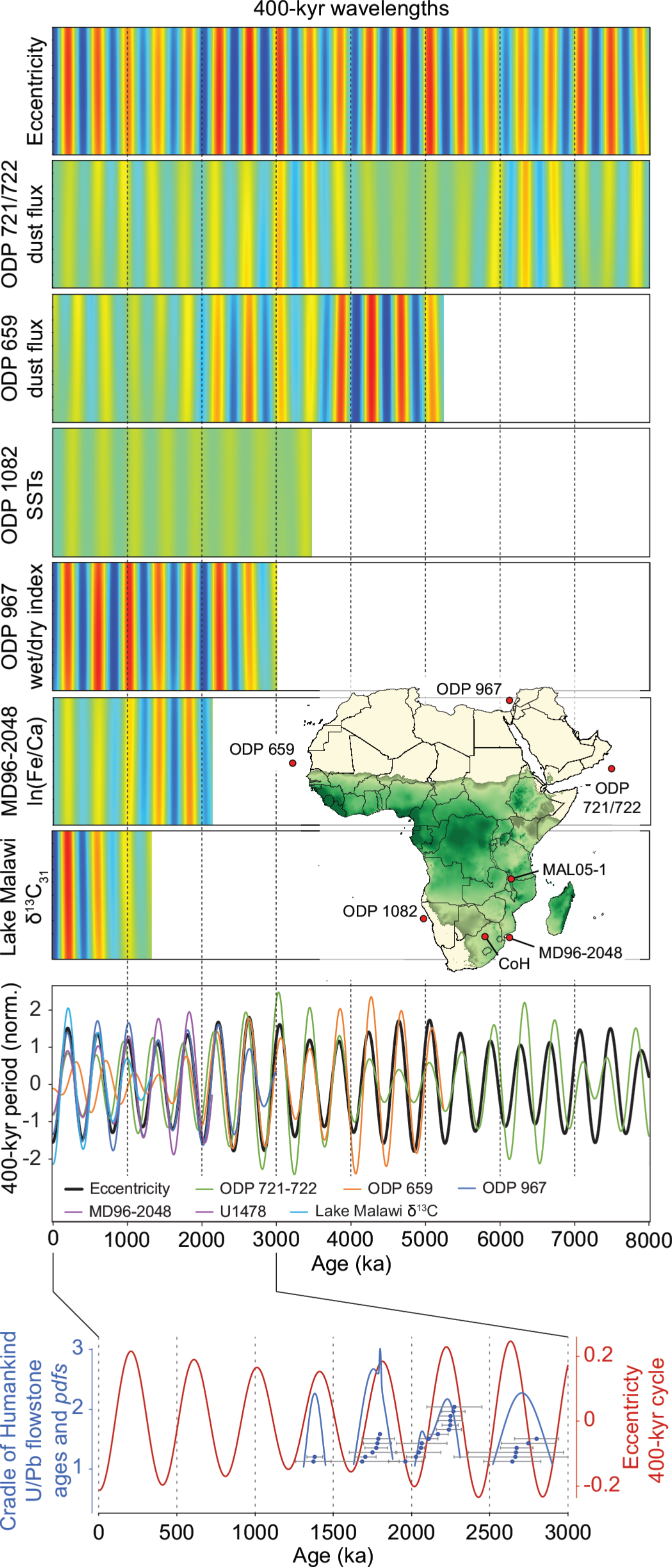

400-kyr wavelengths
Eccentricity
ODP 721/722 dust flux
ODP 659 dust flux
ODP 1082 SSTs
ODP 967 wet/dry index
MD96-2048 ln(Fe/Ca)
Lake Malawi $\delta^{13}C_{31}$
ODP 967
ODP 659
ODP 721/722
MAL05-1
ODP 1082
MD96-2048
CoH
400-kyr period (norm.)
Eccentricity
ODP 721-722
ODP 659
ODP 967
MD96-2048
U1478
Lake Malawi $\delta^{13}C$
Age (ka)
Cradle of Humankind U/Pb flowstone ages and *pdfs*
Eccentricity 400-kyr cycle
Age (ka)

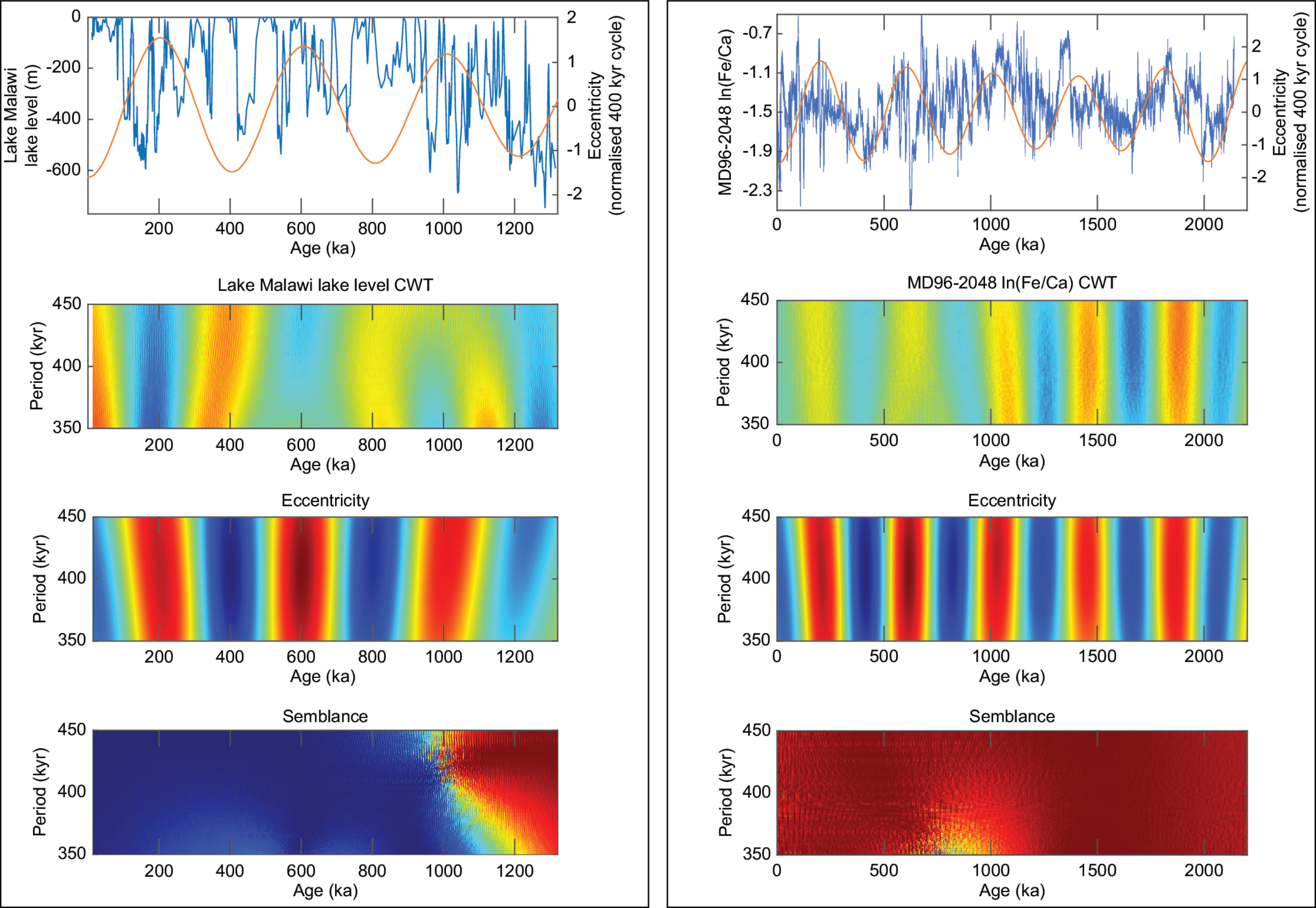

Lake Malawi lake level (m)
Eccentricity (normalised 400 kyr cycle)
Age (ka)
Lake Malawi lake level CWT
Period (kyr)
Eccentricity
Semblance
MD96-2048 ln(Fe/Ca)
MD96-2048 ln(Fe/Ca) CWT

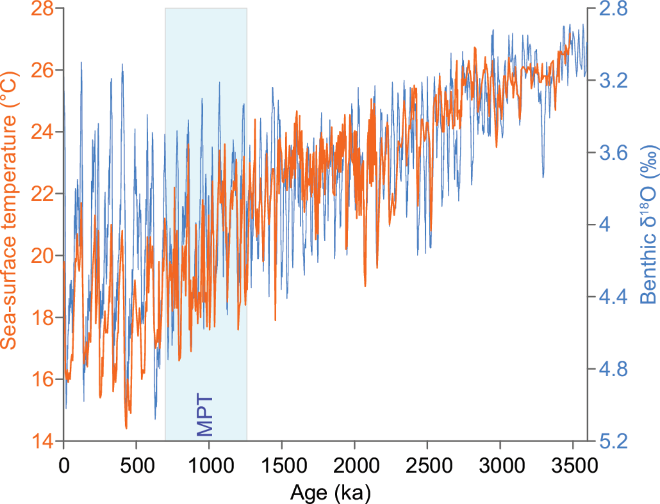
28
26
24
22
20
18
16
14
Sea-surface temperature (°C)
2.8
3.2
3.6
4
4.4
4.8
5.2
Benthic δ18O (‰)
MPT
0
500
1000
1500
2000
2500
3000
3500
Age (ka)

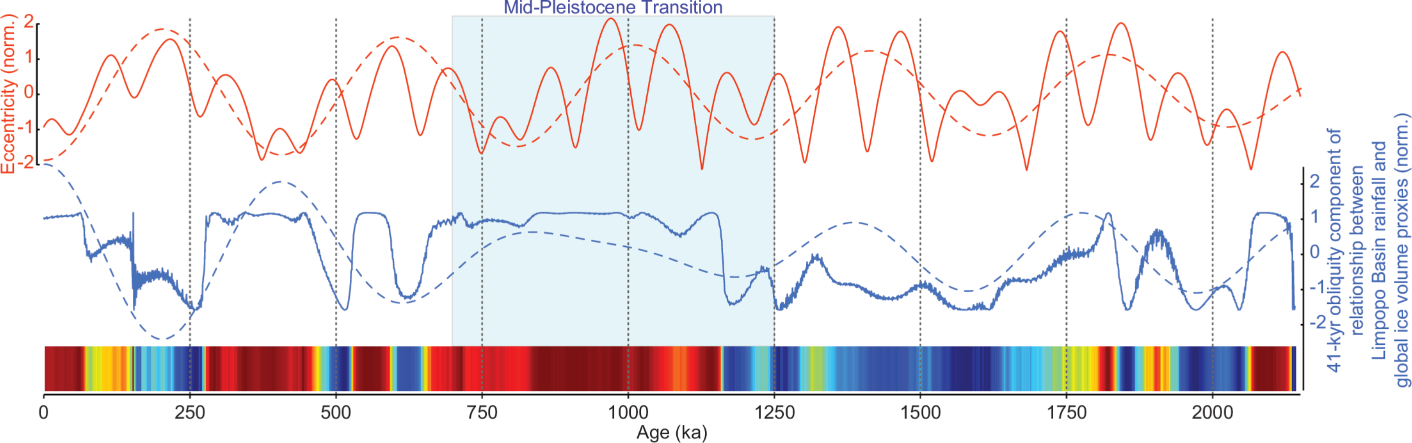
Mid-Pleistocene Transition
Eccentricity (norm.)
2
1
0
-1
-2
41-kyr obliquity component of relationship between Limpopo Basin rainfall and global ice volume proxies (norm.)
2
1
0
-1
-2
0
250
500
750
1000
1250
1500
1750
2000
Age (ka)

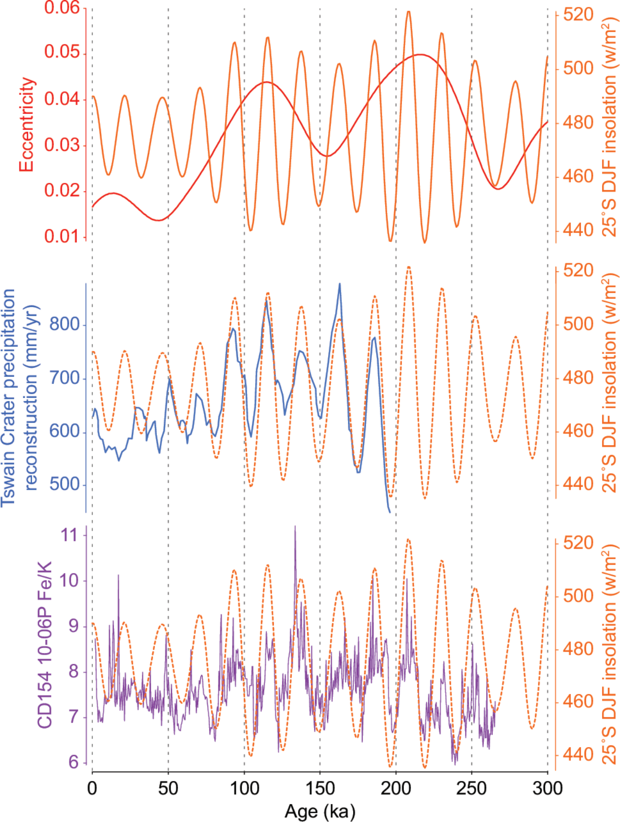

Eccentricity
0.06
0.05
0.04
0.03
0.02
0.01
25˚S DJF insolation (w/m²)
520
500
480
460
440
Tswain Crater precipitation reconstruction (mm/yr)
800
700
600
500
CD154 10-06P Fe/K
11
10
9
8
7
6
0
50
100
150
200
250
300
Age (ka)

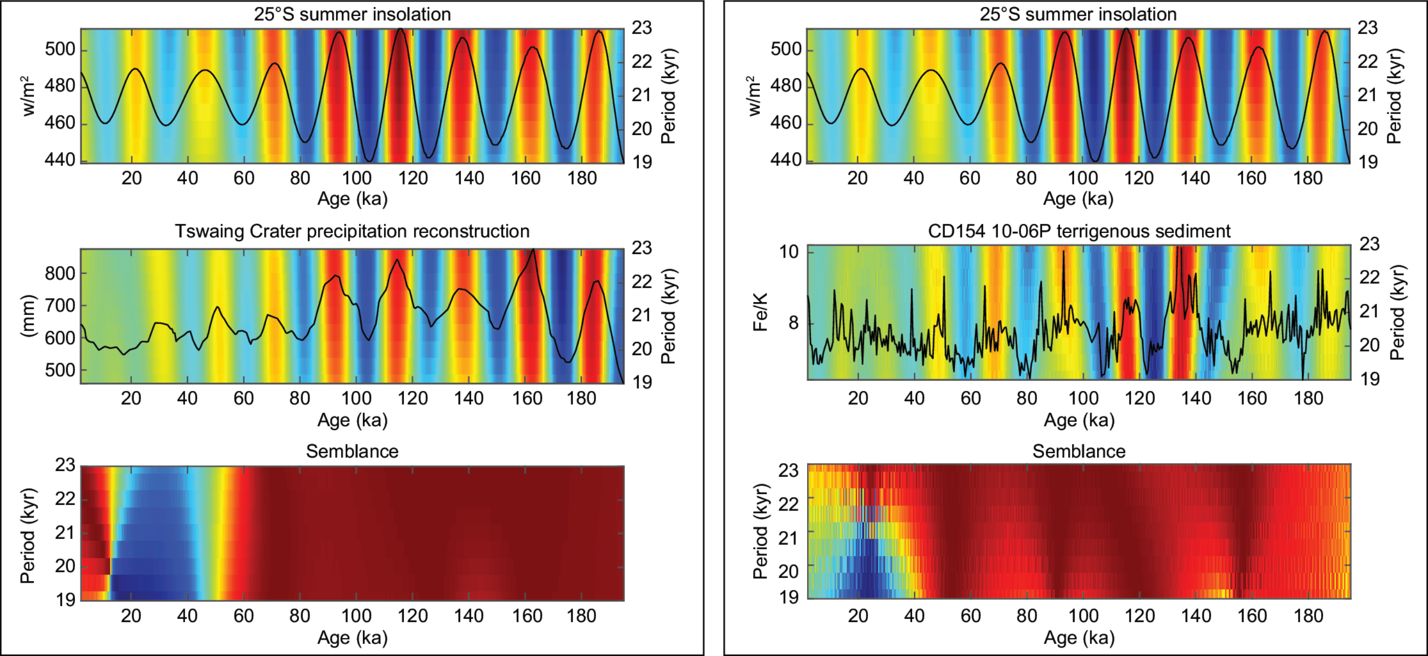
25°S summer insolation
w/m²
440
460
480
500
Period (kyr)
19
20
21
22
23
Age (ka)
20
40
60
80
100
120
140
160
180
Tswaing Crater precipitation reconstruction
(mm)
500
600
700
800
Semblance
25°S summer insolation
CD154 10-06P terrigenous sediment
Fe/K
8
10
Semblance

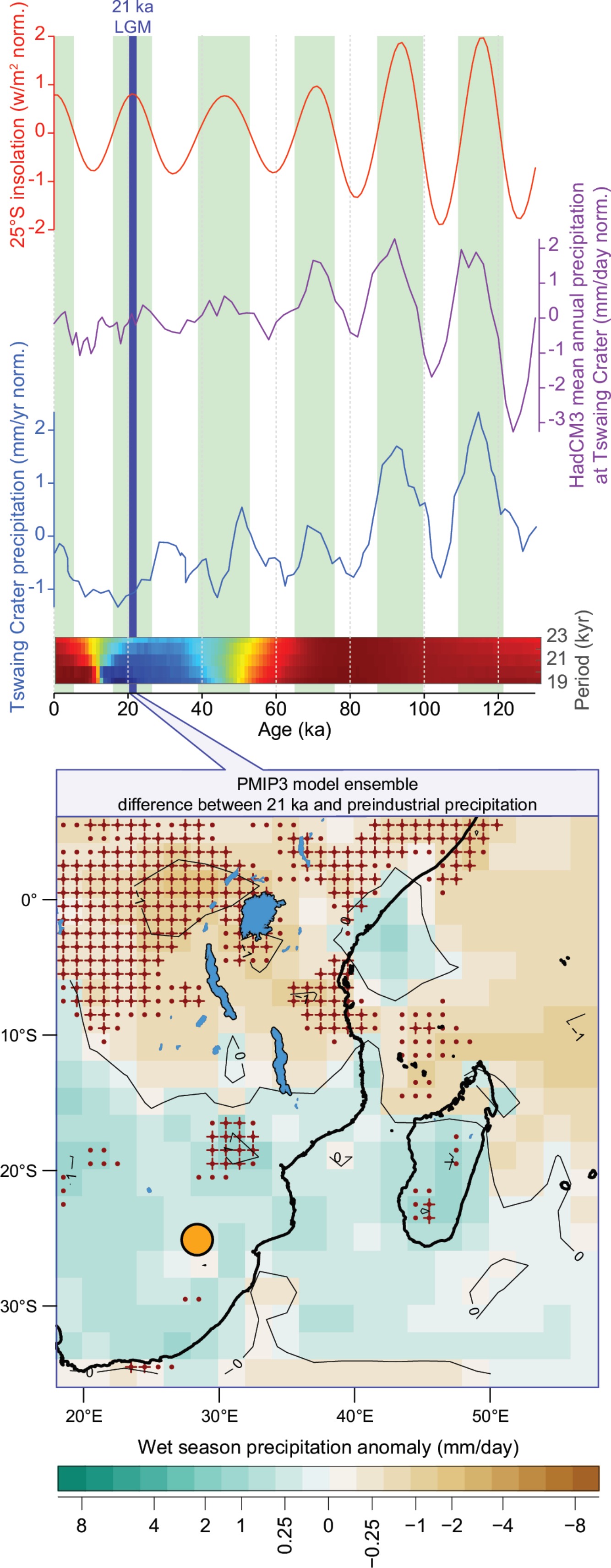

21 ka
LGM
25°S insolation (w/m² norm.)
HadCM3 mean annual precipitation at Tswaing Crater (mm/day norm.)
Tswaing Crater precipitation (mm/yr norm.)
Period (kyr)
Age (ka)
PMIP3 model ensemble
difference between 21 ka and preindustrial precipitation
0°
10°S
20°S
30°S
20°E
30°E
40°E
50°E
Wet season precipitation anomaly (mm/day)
8
4
2
1
0.25
0
−0.25
−1
−2
−4
−8

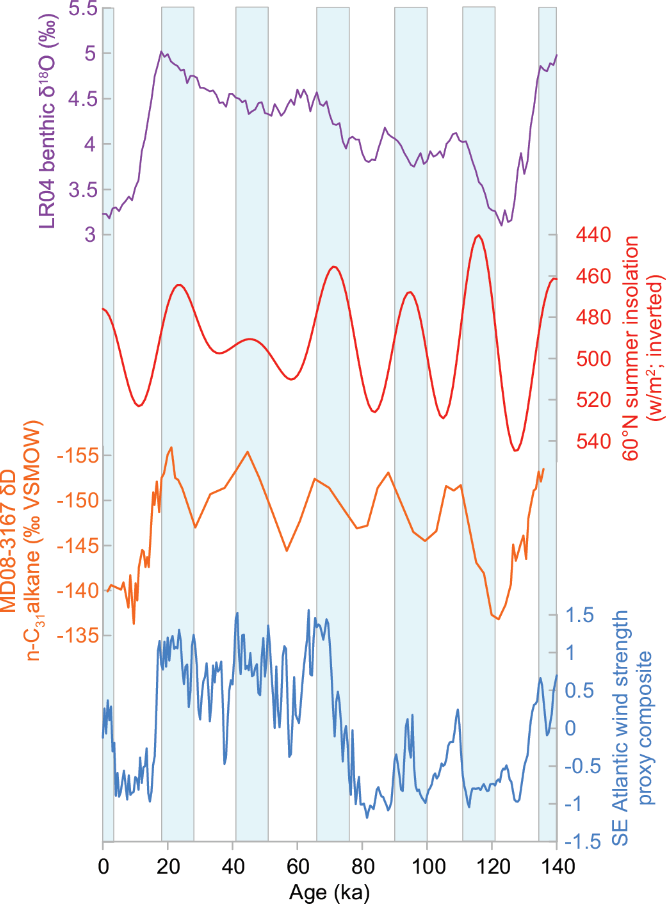

LR04 benthic δ18O (‰)
5.5
5
4.5
4
3.5
3
440
460
480
500
520
540
60°N summer insolation (w/m2; inverted)
-155
-150
-145
-140
-135
MD08-3167 δD n-C31alkane (‰ VSMOW)
1.5
1
0.5
0
-0.5
-1
-1.5
SE Atlantic wind strength proxy composite
0
20
40
60
80
100
120
140
Age (ka)